

1-31-1990

Dioxin formation : thermodynamics and reaction pathways during the oxidation/incineration of chloroaromatics

Sanjiv Narendra Patel
New Jersey Institute of Technology

Follow this and additional works at: <https://digitalcommons.njit.edu/theses>

 Part of the [Chemical Engineering Commons](#)

Recommended Citation

Patel, Sanjiv Narendra, "Dioxin formation : thermodynamics and reaction pathways during the oxidation/incineration of chloroaromatics" (1990). *Theses*. 1921.
<https://digitalcommons.njit.edu/theses/1921>

This Thesis is brought to you for free and open access by the Electronic Theses and Dissertations at Digital Commons @ NJIT. It has been accepted for inclusion in Theses by an authorized administrator of Digital Commons @ NJIT. For more information, please contact digitalcommons@njit.edu.

Copyright Warning & Restrictions

The copyright law of the United States (Title 17, United States Code) governs the making of photocopies or other reproductions of copyrighted material.

Under certain conditions specified in the law, libraries and archives are authorized to furnish a photocopy or other reproduction. One of these specified conditions is that the photocopy or reproduction is not to be “used for any purpose other than private study, scholarship, or research.” If a user makes a request for, or later uses, a photocopy or reproduction for purposes in excess of “fair use” that user may be liable for copyright infringement,

This institution reserves the right to refuse to accept a copying order if, in its judgment, fulfillment of the order would involve violation of copyright law.

Please Note: The author retains the copyright while the New Jersey Institute of Technology reserves the right to distribute this thesis or dissertation

Printing note: If you do not wish to print this page, then select “Pages from: first page # to: last page #” on the print dialog screen

The Van Houten library has removed some of the personal information and all signatures from the approval page and biographical sketches of theses and dissertations in order to protect the identity of NJIT graduates and faculty.

ABSTRACT

Title of Thesis : Dioxin Formation: Thermodynamics and reaction pathways during the incineration/oxidation of chloroaromatics

Sanjiv Patel, Master of Science in Chemical Engineering,
1990

Thesis directed by: Dr. Joseph Bozzelli
Prof. Dept. of Chemistry, Chemical
Engg. and Environmental Science.
New Jersey Institute of Technology

Enthalpy, entropy and heat capacity property estimation for cyclic molecules using Benson's group additivity method require the use of ring correction terms. Ring correction terms are estimated from the thermodynamic properties of the cyclic molecule being considered. In the absence of literature values a procedure is proposed to predict these thermodynamic values.

Benson's Group additivity method does not fully account for the interactions between bulky group or atom substituents on the aromatic ring. In order to have accurate thermo-

dynamic properties for these compounds, a data base is generated with ortho, meta and para interactions for (Cl-Cl), (Cl-OH), (OH-OH), (CH₃-CH₃), (CH₃-OH) and (F-F) to be used with Benson's group method. In case of three or more methyls, buttress effect to be used has been included. In case of multiply substituted aromatics a counting scheme is proposed to obtain effective number of interactions.

The ring correction groups and group interactions are used with Benson' group method to predict thermodynamic properties of likely candidate precursors to dioxin formation during the oxidation/incineration of chloroaromatics. Based on these thermodynamic properties a set of reaction pathways is proposed which could lead to the formation of dioxins. A comparison is carried out between reaction systems with chlorine substituents with similar systems without chlorines to explain larger formation of chlorinated dioxins. Quantum Rice-Ramsperger-Kassel calculations for determining kinetic (rate constants) are carried out for select pathways.

DIOXIN FORMATION: THERMODYNAMICS AND REACTION PATHWAYS
DURING THE OXIDATION/INCINERATION OF CHLOROAROMATICS

by

Sanjiv Patel

Thesis submitted to the Faculty of the Graduate School of
the New Jersey Institute of Technology in partial
fulfillment of the requirements for the degree of
Master of science in Chemical Engineering
1990

APPROVAL SHEET

Title of Thesis: Dioxin formation: thermodynamics and
reaction pathway during the oxidation/
incineration of chloroaromatics

Name of Candidate: Sanjiv Patel
Master of Science in Chemical Engineering
1990

Thesis and abstract approved:

Joseph Bozzelli 11/90
Professor
Department of Chemistry,
Chemical Engineering and
Environmental Science

(Dr. Henry Shaw) 1/11/90

(Dr. Dana Knox) 1/11/90

VITA

Name: Sanjiv Narendra Patel

Permenant address:

Date of birth:

Place of birth:

Secondary education: Mithibai College, Bombay, April 1980

Collegiate institution attended	Dates	Degree	Date of degree
New Jersey Institute of Technology	Fall 87 to Fall 90	MSChE	January 1990
Indian Institute of Technology, Kanpur	May 83 to May 87	BTech ChE	June 87

Major: Chemical Engineering

Positions held: Simulation Engineer
Autodynamics
100 Willowbrook road
Freehold, NJ 07728

TABLE OF CONTENTS

Chapter	page
I. ESTIMATION OF RING CORRECTION GROUPS	1
II. ESTIMATION OF GROUP INTERACTION TERMS FOR AROMATIC RINGS	13
III. REACTION PATHWAYS LEADING TO THE FORMATION OF DIOXINS AND DIBENZOFURANS	22
IV. QUANTUM RICE-RAMSPERGER-KASSEL ANALYSIS FOR REACTION PATHWAYS	32
APPENDIX A. RING CORRECTION GROUPS	47
APPENDIX B. GROUP INTERACTION TERMS FOR AROMATIC RINGS AND PREDICTED VALUES	52
APPENDIX C. REACTION ANALYSIS OUTPUT	54
APPENDIX D. QRRK INPUT PARAMETERS	56
APPENDIX E. ENERGY LEVEL DIAGRAMS AND THERMODYNAMIC DATA	59
APPENDIX F. QRRK ANALYSIS OUTPUT GRAPHS	76
APPENDIX G: COMPUTER INPUTS FOR QRRK ANALYSIS	91
APPENDIX H: SYNOPSIS FOR CHAPTERS I TO III	101
REFERENCES	103

ESTIMATION OF RING CORRECTION GROUPS

Introduction

Ring correction terms or ring correction groups for use in the group additivity method of molecular thermodynamic property estimation for ring compounds are the differences between the known or experimental thermodynamic property of the molecule and the sum of value calculated from Benson¹⁻³ groups that the equivalent noncyclic molecular isomer is composed of. The ring correction groups usually contain significant entropy and enthalpy corrections with smaller corrections in heat capacities. These deviations between cyclic and non cyclic molecular properties result from interactions such as ring strain, loss of internal rotations and increased bending vibrational (and puckering) modes. An example is cyclopropane, which is made up of 3 C/C2/H2 groups which are developed from linear hydrocarbon molecules that do not have any ring strain and which have significant internal rotations around the C-C bonds. To use the group additivity scheme for cyclopropane one needs to sum the thermodynamic data for the 3 C/C2/H2 groups, plus include (add) a ring correction term⁽²⁾. While this may be more complex than calculation for non cyclic compounds, it is more straight

forward than having a completely separate set of needed groups for each size ring compound .

Estimation of ring corrections for hydrocarbons

Thermodynamic properties for cyclic hydrocarbon rings with eight or fewer carbon atoms have been published by Dorofeeva et al.(4). We have used these literature values with the group and symmetry assignment data of Benson(3) to calculate the ring corrections needed for use by the group additivity method. Enthalpy and Entropy values represent properties of formation at 298 K.

The entropy corrections were estimated based on experimental or actual entropy and the intrinsic entropy. Intrinsic entropy $S_{\text{intrinsic}}$ is defined as

$$S_{\text{parent molecule}} = S_{\text{intrinsic}} - R \cdot \ln(\sigma) + R \cdot \ln(\sigma_I)$$

Ring correction for entropy is therefore the difference between the intrinsic entropy from experiment and that calculated from the corresponding nonring groups. The intrinsic entropy of the ring is obtained from Dorofeeva et al(4). Entropy which does not include the symmetry correction $R \cdot \ln(\sigma)$ was used to calculate the ring correction terms. The intrinsic entropy was calculated from the above equation

Enthalpy terms were estimated by taking the difference between the known or calculated enthalpy of formation of the molecule and the sum of the contributing groups. ΔH_{RC} for example:

$$\Delta H_{\text{RC}} = H_{\text{parent molecule}} - \sum_{i=1}^n H_i$$

for n contributing groups.

Heat capacities were calculated in the same manner as enthalpy, only using corresponding molecule and group values for heat capacity.

The resultant ring correction groups for hydrocarbons are given in table I. In the case of cyclopentane and cycloheptane, different symmetry numbers of 10 vs 1 and 1 vs 2 have been given by Benson⁽³⁾ and Dorofeeva⁽¹⁾, respectively. Thus the entropy correction terms are different depending on the symmetry number used in the calculation of intrinsic entropy. Table 1 lists corrections with both values of symmetry.

SAMPLE CALCULATION

A sample calculation for 1,5-cyclooctadiene is shown below using group data from Benson⁽³⁾. We use the notation C/C2/H2 which presents the adjacent atoms in alphabetical order instead of the Benson terminology of C/H2/C2 because we have instituted this terminology in the THERM⁽⁵⁾ computer program for the calculations using group additivity and data manipulation into NASA and list data formats as well as reaction thermodynamics property calculations. Literature data is from Dorofeeva⁽⁴⁾ and is denoted by superscript parenthesis

$$\begin{aligned} H_{GA} &= \sum_{i=1}^3 H_i \quad \text{where } i=8 \text{ for 8 central carbon atoms} \\ &= 4 * H_{CD/C/H} + 4 * H_{C/C/CD/H2} \\ &= 4 * 8.59 + 4 * (- 4.76) \\ &= 15.32 \text{ kcal/mol} \end{aligned}$$

$$\begin{aligned}
 S_{GA} &= \sum_{i=1}^8 S_i - R * \ln(\sigma) \quad (\text{cyC82e-15}) \sigma = 2 \\
 &= 4 * S_{CD/C/H} + 4 * S_{C/C/CD/H2} - 1.98 * \ln(2) \\
 &= 4 * 7.97 + 4 * 9.80 - 1.987 * \ln(2) \\
 &= 69.70 \text{ cal/mol-K}
 \end{aligned}$$

$$\begin{aligned}
 CP_{GA} &= \sum_{i=1}^8 CP_i \quad \text{for } Cp_{300} \text{ k} \\
 &= 4 * CP_{CD/C/H} + 4 * CP_{C/C/CD/H2} \\
 &= 4 * 4.16 + 4 * 5.12 \\
 &= 37.12 \text{ cal/mol-K}
 \end{aligned}$$

$$\begin{aligned}
 H_{RC} &= H^{(4)} - H_{GA} \\
 &= 14.02 - 15.32 \\
 &= -1.3 \text{ kcal/mol}
 \end{aligned}$$

$$\begin{aligned}
 S_{RC} &= S^{(4)} - S_{GA} + R * \ln(\sigma) \\
 &= 83.85 - 69.7 + 1.987 * \ln(2) \\
 &= 12.77 \text{ cal/mol-K}
 \end{aligned}$$

$$\begin{aligned}
 300 \text{ K } CP_{RC} &= CP^{(4)} - CP_{GA} \\
 &= 33.31 - 37.12 \\
 &= -3.81 \text{ cal/mol-K}
 \end{aligned}$$

HYDROCARBON MOLECULES WITH OXYGEN IN THE RING

Experimental thermodynamic data for hydrocarbons with less than four carbons and an oxygen in the ring (oxiranes) can be obtained from the literature^(2,3,6). However, for larger molecules (cyclic C₄O and above), there is very little data available. We therefore needed to devise a method for the estimation of the thermodynamic properties of such molecules in order to estimate their ring corrections.

We estimated the properties of these cyclic ethers by observing trends in the differences between thermodynamic properties of linear hydrocarbons and corresponding linear ethers. Differences in the heat capacities⁽²⁾ between CCC and COC, or CCCC and CCOC, or CCCCC and CCOCC etc are found to be constant for a particular temperature. This is, in fact, one of the principles on which the group additivity method of calculating thermodynamic parameters is based. If this difference is then assumed to be the same as between a ring hydrocarbon and a ring hydrocarbon ether (oxygen substituted for a carbon), then the heat capacity of the oxygen containing ring can be calculated using this difference value.

In cases where the specific heats are not in the literature, the procedure described above can be used. An example of such a calculation is shown below and gives specific heats which are in good agreement with those given in Stull⁽⁶⁾.

SAMPLE CALCULATIONS

$$\begin{aligned} & \triangle^c \text{ Cyc20} & \sigma = 2 \\ H_{RC} \text{ Cyc20} &= H^{(2)}_{\text{Cyc20}} - H_{GA} \text{ Cyc20} \\ &= -12.58 - (-39.40) \\ &= 26.82 \text{ kcal/mol} \\ \Delta S &= S_{CCC}^{(6)} - S_{COC}^{(6)} \\ &= 0.68 \text{ cal/mol-K} \\ S_{\text{Cyc20}} &= \Delta S + S_{\text{Cyc3}}^{(4)} + R \cdot \ln\left(\frac{\sigma_{\Delta}}{\sigma_{\text{Cyc}}}\right) - R \cdot \ln\left(\frac{\sigma_{\text{Cyc}}}{\sigma_{\Delta}}\right) \end{aligned}$$

$$= 58.30 \text{ cal/mol-K}$$

$$S_{RC \text{ cyc}20} = S_{\text{cyc}20} - S_{GA \text{ cyc}20} + R \cdot \ln(2) \\ = 31.39 \text{ cal/mol-K}$$

$$\Delta CP = CP_{CCC}^{(6)} - CP_{COC}^{(6)}$$

$$CP_{\text{cyc}20} = CP_{\text{cyc}3}^{(4)} - \Delta CP$$

$$CP_{RC \text{ cyc}20} = CP_{\text{cyc}20} - CP_{GA \text{ cyc}20}$$

The differences in enthalpy, entropy and heat capacities⁽⁶⁾ between CCCCC & CCOCC, or CCCCCC & CCCOCC, etc., become almost constant for five atoms or more in the chain. These differences are shown below

$$H_{CCCCCC} - H_{CCCOCC} = 25.12 \text{ kcal/mol}$$

$$S_{CCCCCC} - S_{CCCOCC} = 1.290 \text{ cal/mol-K}$$

$$300 \text{ K } CP_{CCCCCC} - CP_{CCCOCC} = 1.87 \text{ cal/mol-K}$$

$$500 \text{ K } CP_{CCCCCC} - CP_{CCCOCC} = 4.81 \text{ cal/mol-K}$$

$$800 \text{ K } CP_{CCCCCC} - CP_{CCCOCC} = 7.04 \text{ cal/mol-K}$$

$$1000 \text{ K } CP_{CCCCCC} - CP_{CCCOCC} = 8.05 \text{ cal/mol-K}$$

An example for the estimation of properties for cyc70 is shown below.

Estimation for  (cyc70)

$$H_{\text{cyc}70} = H_{\text{cyc}8}^{(4)} - (H_{CCCOCC} - H_{CCCCCC}) \\ = -29.73 - 25.12 \\ = -54.85 \text{ kcal/mol}$$

$$H_{RC \text{ cyc}70} = H_{\text{cyc}70} - H_{GA \text{ cyc}70} \\ = -54.85 - (-64.02)$$

$$\begin{aligned}
&= -9.17 \text{ kcal/mol} \\
S_{\text{cyC70}} &= S_{\text{cyC8}}^{(4)} - (S_{\text{cccoccc}} - S_{\text{ccccccc}}) + R \ln\left(\frac{\sigma}{\sigma_0}\right) \\
&\quad - R \ln\left(\frac{\sigma}{\sigma_0}\right) \\
&= 87.86 - 1.290 + 0.0 - 0.0 \\
&= 86.57 \text{ kcal/mol-K} \\
S_{\text{RC cyC70}} &= S_{\text{cyC70}} - S_{\text{GA cyC70}} \\
&= 86.57 - 75.25 \\
&= 11.06 \text{ cal/mol-K}
\end{aligned}$$

300 K

$$\begin{aligned}
C_{\text{PcyC70}} &= C_{\text{PcyC8}}^{(4)} - (C_{\text{Pcccoccc}} - C_{\text{Pccccccc}}) \\
&= 35.18 - 1.870 \\
&= 33.31 \text{ cal/mol-K} \\
C_{\text{PRC cyC70}} &= C_{\text{PcyC70}} - C_{\text{P GA cyC70}} \\
&= 33.31 - 40.85 \\
&= -7.54 \text{ cal/mol-K}
\end{aligned}$$

A list of ring corrections for oxygen containing rings without double bonds are given in table II.

UNSATURATED HYDROCARBONS WITH OXYGEN IN THE RING

The thermodynamic properties of these molecules are estimated using a similar procedure to the case of saturated oxygen rings. Here differences in thermodynamic properties between hydrocarbon rings with and without a double bond are used to estimate the corresponding properties of an unsaturated oxygen containing ring. Resonance between a double bond and an oxygen atom will

tend to lower the enthalpy of formation. This effect is accounted for by assuming that the difference in enthalpy with and without resonance correction is the same as that between an ether molecule having a corresponding atom and double bond arrangement to an olefin with same number of carbon atoms, and adding this to the estimated property.

Estimation for enthalpy of formation of an oxygen containing unsaturated cyclic molecule is shown below

ESTIMATION FOR

$$\Delta H = H^{(4)}_{\text{cyC51e}} - H^{(4)}_{\text{cyC5}}$$

$$H_{\text{cyC401e-1}} = H^{(6)}_{\text{cyC40}} + \Delta H + \text{RS1}$$

where RS1 is the resonance correction for the oxygen containing ring. $H_{\text{cyC401e-1}}$ is the enthalpy of formation of dihydrofuran. The nomenclature used here is:

cy : cyclic compound

C40 : five membered ring with oxygen

1e : one double bond

-1 : position of double bond in the ring

The RS1 value is be estimated by:

$$\begin{aligned} \Delta H1 &= H_{\text{CCOCC}} - H_{\text{CCCCC}} \\ &= -25.26 \text{ kcal/mol} \end{aligned}$$

$$\begin{aligned} \Delta H2 &= H_{\text{C*COCC}} - H_{\text{C*CCCC}} \\ &= -28.63 \text{ kcal/mol} \end{aligned}$$

$$\begin{aligned} \text{RS1} &= \Delta H2 - \Delta H1 \\ &= -3.37 \text{ kcal/mol} \end{aligned}$$

Ring corrections for  (cyC502e-14) can be obtained by

$$\Delta H = H^{(4)}_{\text{cyC62e-14}} - H^{(4)}_{\text{cyC52e}}$$

$$H_{\text{cyC502e-14}} = H^{(6)}_{\text{cyC502e}} + \Delta H + \text{RS2}$$

where RS2 is the resonance correction for oxygen containing ring with two double bonds. Its value is estimated by:

$$\begin{aligned} \Delta H3 &= H_{\text{C*COc*c}} - H_{\text{C*CCC*c}} \\ &= -28.51 \text{ kcal/mol} \end{aligned}$$

$$\begin{aligned} \text{RS2} &= \Delta H3 - \Delta H1 \\ &= -3.25 \text{ kcal/mol} \end{aligned}$$

Entropy and heat capacity are estimated as described in saturated oxygen ring compound section.

The procedure shown above for resonance interaction can also be used to obtain the ring corrections for  (cyC502e-13) and other diene rings using resonance corrections as shown above.

A list of corrections for cyclic olefinic molecules with oxygen is given in table III.

ESTIMATION OF RING CORRECTIONS FOR SATURATED RINGS WITH NITROGEN

Literature data are available^(3,6) for cyclic molecules with nitrogen in the ring (cyC3N and smaller) and so our calculations use this data. For larger molecules the technique for enthalpy, entropy and heat capacity as described in the saturated oxygen case is used. The differences in the properties between linear nitrogen

containing molecule (amines) and a hydrocarbons with same number of central atoms are observed to be constant. These differences are then used to estimate the properties of the nitrogen containing rings and can be written as:

$$\Delta H = H_C \text{ RING} - H_N \text{ RING} = - 17.7 \text{ kcal/mol}$$

$$\Delta S = S_C \text{ RING} - S_N \text{ RING} = - 0.87 \text{ cal/mol-K}$$

$$300 \text{ K} \quad C P_C \text{ RING} - C P_N \text{ RING} = 1.08 \text{ cal/mol-K}$$

$$500 \text{ K} \quad C P_C \text{ RING} - C P_N \text{ RING} = 2.09 \text{ cal/mol-K}$$

$$800 \text{ K} \quad C P_C \text{ RING} - C P_N \text{ RING} = 3.14 \text{ cal/mol-K}$$

$$1000 \text{ K} \quad C P_C \text{ RING} - C P_N \text{ RING} = 3.64 \text{ cal/mol-K}$$

A list of nitrogen ring correction groups is given in table IV

UNSATURATED HYDROCARBON MOLECULES WITH NITROGEN IN THE RING

The procedure is the same as in the case with oxygen in the ring. Resonance corrections are taken to be the same as in the oxygen case. Two ring corrections are given in table V.

HYDROCARBON MOLECULES WITH SULFUR IN THE RING

Experimental data for cyclic molecules with sulfur in the ring are given in the literature⁽⁶⁾. Using these values and those obtained by the group method, the ring corrections can be estimated. For an eight membered ring, the thermodynamic properties are not available, and so were

estimated using a procedure similar to the one described for the oxygen case. The constant differences between the linear molecules is given below

$$HCCCCSCCC - HCCCCCCCC = 14.94 \text{ kcal/mol}$$

$$SCCCCSCCC - SCCCCCCCC = 4.967 \text{ cal/mol-K}$$

$$300 \text{ K } CpCCCCSCCC - CpCCCCCCCC = -1.15 \text{ cal/mol-K}$$

$$500 \text{ K } CpCCCCSCCC - CpCCCCCCCC = -2.93 \text{ cal/mol-K}$$

$$800 \text{ K } CpCCCCSCCC - CpCCCCCCCC = -2.99 \text{ cal/mol-K}$$

$$1000 \text{ K } CpCCCCSCCC - CpCCCCCCCC = -2.22 \text{ cal/mol-K}$$

A list of ring correction groups for rings with sulfur is given in table VI.

ESTIMATION OF RING CORRECTIONS FOR OLEFINIC MOLECULES WITH SULFUR IN THE RING

The procedure for the estimation of ring corrections with sulfur in the ring is the same as in the case of an olefinic ring with oxygen in the ring. Resonance corrections are taken to be the same as in the oxygen case. A list of ring corrections is given in table VII.

SYMBOLS

- H_{RC} : Ring correction for enthalpy in kcal/mol
- S_{RC} : Ring correction for entropy in cal/mol-K
- CP_{RC} : Ring correction for specific heats cal/mol-K
- H_{GA} : Enthalpy from group method in kcal/mol
- S_{GA} : Entropy from group method in cal/mol-K
- CP_{GA} : Specific heat from group method in cal/mol-K
- σ : Symmetry number of the molecule
- O_I : Number of optical isomers

ESTIMATION OF GROUP INTERACTION TERMS FOR AROMATIC RINGS

Introduction

Chlorinated dibenzodioxins and dibenzofurans are often observed in effluents from oxidation or incineration of chlorinated aromatics such as chlorinated benzenes, biphenyls, and phenols(8). These compounds are thought to be highly toxic, and as a consequence, are highly undesirable products of incomplete combustion (PIC's). It would be of significant value to have an accurate and fundamental understanding of the mechanism for their formation, in addition to knowledge of their thermodynamic properties in order to work toward the goal of eliminating these species from effluent streams. One possible use for this information could be to incorporate it into a detailed mechanism which models the incineration process. This model could then be utilized for prediction and/or feedback control to optimize conversion of the various feed carbon and chlorine species towards desired products, such as CO_2 , H_2O and HCl , and to suppress dibenzodioxin formation.

Very little has been published on the thermodynamic properties and elementary reactions which lead to formation of dioxins and chlorinated dioxins. Benson's group method(1-3,4), when used for the estimation of thermodynamic properties of molecules, does not account for all interactions between functional groups or atoms on

aromatics, such as ortho, meta or para interactions of methyls or chlorines. It is often necessary to correct values obtained using group additivity for interactions between these substituents. To obtain correction values, one may use the differences between literature thermodynamic values(7,9-16) and those obtained using group additivity. Due to the limited literature data, however, one must often proceed by obtaining the corrections based on known properties for only a few molecules and then apply these to more complex species. This has been previously demonstrated by Shaub (17,18) for chloro and oxy substituted aromatics.

As an initial step towards the development of a detailed mechanism describing chlorinated dioxin formation, we have developed improved values for groups representing non-next-nearest neighbor contributions from substituents on aromatic rings, such as Cl, F, OH, CH₃O, CH₃, and COOH (acid group). We utilize these group values to calculate thermodynamic properties for a number of chlorinated dibenzodioxins, dibenzofurans, and likely radical precursors to chlorinated dibenzodioxin and dibenzofuran formation.

Procedure

If the thermodynamic properties of the molecule being considered are known from experiments, then interaction groups can be calculated as the difference between experimental and group additivity property values(1,3). The group additivity values are summed by using a computer code called THERM(5). To compute the non-next-nearest neighbor

correction for ortho (Cl-Cl) on an aromatic ring, for example, the following procedure is used:

$$X_{(\text{Cl-Cl})\text{Ortho}} = X_{\text{Expt}} - X_{\text{Ga}}$$

where X represents the enthalpy, entropy or heat capacity interaction values

X_{Expt} is the corresponding experimental or literature value

X_{Ga} is the group additivity value obtained by summing the constituent groups of the molecule

Groups determined in this way represent interactions between substituents in the ortho, meta or para positions. They are applied to Benson's group additivity formalism as corrections (an additional group). A list of interaction groups we determined is given in Table VIII.

We note that these group values are optimized for disubstituted single ring aromatics and need to be adjusted in order to give good estimates for poly-substituted aromatics. We observed that the use of interaction groups derived in this fashion to calculate values for poly-substituted aromatics gave predictions which were consistently in error. This results from the fact that poly-substituted aromatics do not simply have ortho, meta, and para interactions; they are more complex. We, therefore, developed a method for counting the number of interactions when there are more than two substituents. The scheme we recommend for thermodynamic property estimates on

these species uses interaction groups derived in this work, and can be illustrated by considering the example of hexachlorobenzene. This molecule appears to have 6 ortho Cl/Cl, 6 meta Cl/Cl and 3 para Cl/Cl interactions, however, counting all of these interactions will result in considerable error. Therefore, we count the effective number of ortho, meta, and para interactions which give reasonable property estimates. This method maintains the simplicity of the group additivity approach. We empirically determined that considering all ortho but only half the number of meta and/or para interactions gives reasonable predictions (compared to experimental data) for poly-substituted aromatic species. We also round off to the lower integer fractional meta or para interactions. In this way, we weight ortho, meta, and para effects in order to obtain accurate thermodynamic property estimates. This method was derived by comparison of calculated values for polysubstituted benzenes such as hexachlorobenzene, to published data and only applies to species which have more than one type of interaction.

The effective number of interactions for hexachlorobenzene is then given as follows:

6 ortho, 3 meta and 1 para.

$$X_{C_6Cl_6} = X_{Ga} + 6 X_{(Cl-Cl)ortho} + 3 X_{(Cl-Cl)meta} + 1 X_{(Cl-Cl)para}$$

$$H_{C_6Cl_6} = H_{Ga} + 6 H_{(Cl-Cl)ortho} + 3 H_{(Cl-Cl)meta} + 1 H_{(Cl-Cl)para}$$

$$= -24.66 + 6 (2.18) + 3 (1.34) + 0.52$$

$$= -7.04 \text{ kcal/mol}$$

$$H_{C6Cl6} = -8.1 \text{ kcal/mol as given by Stull(6)}$$

$$S_{C6Cl6} = S_{Ga} + 6 S_{(Cl-Cl)ortho} + 3 S_{(Cl-Cl)meta} \\ + 1 S_{(Cl-Cl)para}$$

$$= 107.74 + 6 (-0.31) + 3 (0.17) + (-0.08)$$

$$= 106.31 \text{ cal/mol-K}$$

$$S_{C6Cl6} = 105.45 \text{ cal/mol-K as given by Stull(6)}$$

Specific heat at 300 K

$$Cp_{C6Cl6} = Cp_{Ga} + 6 Cp_{(Cl-Cl)ortho} + 3 Cp_{(Cl-Cl)meta} \\ + 1 Cp_{(Cl-Cl)para}$$

$$= 43.02 + 6 (-0.2) + 3 (-0.12) + (-0.1)$$

$$= 41.36 \text{ cal/mol-K}$$

$$Cp_{C6Cl6} = 43.02 \text{ cal/mol-K as given by Stull(6)}$$

Specific heat at 500 K

$$Cp_{C6Cl6} = Cp_{Ga} + 6 Cp_{(Cl-Cl)ortho} + 3 Cp_{(Cl-Cl)meta} \\ + 1 Cp_{(Cl-Cl)para}$$

$$= 54.96 + 6 (-0.47) + 3 (-0.42) + (-0.36)$$

$$= 50.52 \text{ cal/mol-K}$$

$$Cp_{C6Cl6} = 52.53 \text{ cal/mol-K as given by Stull(6)}$$

This scheme has been applied to chloro, fluoro, hydroxy, ether and methyl substituents on aromatics with resulting estimates that are in good agreement with available literature data.

In the case where there are three or more bulky substituents, such as methyls, on adjacent carbon atoms, an additional correction must be considered to account for restricted rotation of the middle methyl. This correction is termed a Buttress correction or the Buttress effect(13). This is defined as the difference between the experimental property values and the corresponding group additivity estimates which consider ortho, meta and para interactions. Clearly by including corrections we are making the group additivity method more complex, but the increased accuracy outweighs the increased effort.

Estimation involving the Buttress effect is illustrated below:

Consider 1,2,3,4-Tetramethyl Benzene

Number of interactions : 3 (CH₃-CH₃)ortho, 1 (CH₃-CH₃)meta,
0 para and 2 Buttress corrections

$$X_{1,2,3,4\text{-Tetramethyl Benzene}} = X_{Ga} + 3 X_{(\text{CH}_3\text{-CH}_3)\text{ortho}} + 1 X_{(\text{CH}_3\text{-CH}_3)\text{meta}} + 2 X_{\text{Buttress}}$$

Where X is enthalpy, entropy or heat capacity

X_{Ga} Is the property as predicted by the sum of the groups without interaction corrections

Only the integer value of 1/2 the real number of meta and para interactions are used.

The corrections obtained in this work are somewhat different from those obtained by Shaub(16). This is probably due to the f

literature thermodynamic data. We also determined correction values for entropy and heat capacity which are not given by Shaub and are important to estimate ΔG of reaction at varying temperatures.

Table IX compares enthalpy of formation at 298K as predicted using the groups developed in this work for 6 poly-substituted benzenes with predictions from Benson's group values(19) and with literature. Absolute errors between our predictions and literature values range from a low of 0.03 kcal/mol for para cresol to a high of 1.96 kcal/mol for hexamethylbenzene. Predictions of enthalpy using Benson's group values without interactions have somewhat larger absolute errors ranging from 0.35 kcal/mole for p-cresol to 5.93 kcal/mol for hexamethylbenzene.

In Table X, a comparison is made between entropy estimates at 298K and literature values using both interactions derived in this work and Benson's groups alone. Again, better agreement is obtained when we consider the non-next nearest neighbor interactions as described above. Absolute errors range from 0.22 cal/mol-K (low) for hexafluorobenzene to 1.24 (high) cal/mol-K for o-cresol; while estimates using Benson's groups range in absolute error from 0.31 cal/mol-K for hexafluorobenzene to 3.54 cal/mol-K for hexamethylbenzene.

Tables XI and XII compare specific heats at 300 and 500 K using groups developed in this work and those of Benson(3) with some recent literature values. The groups we present give absolute errors at 300 K which range from a

high of 0.83 cal/mol-K for pentamethylbenzene to a low of 0.04 cal/mol-K for m-cresol. Estimates obtained using Benson's groups alone, on the other hand, range from a high of 3.0 cal/mol-K for p-cresol to a low of 0.19 cal/mol-K for pentamethylbenzene. A similar comparison at 500 K yields an absolute error of 3.44 cal/mol-K (high) for hexafluorobenzene and 0.26 cal/mol-K (low) for p-cresol using our groups, while estimates obtained with Benson's groups range in absolute error from 3.8 cal/mol-K (high) for pentamethylbenzene to 0.41 cal/mol-K (low) for p-cresol. Interaction groups presented here are derived from less substituted molecules than those shown in Tables IX, X and XI. The calculated values shown in these tables are in good agreement with available literature data. We feel that the estimates using our groups and calculational procedure are within the error limits of the experimental determinations for referenced thermodynamic properties of these poly-substituted aromatics. We do not suggest that Benson's groups are outside the error limits for these properties, only that our values are closer to the literature data.

Results

A method is developed for estimation of thermodynamic properties of multiplysubstituted aromatics based on principles of group additivity and non-next-nearest neighbor interactions on the aromatic ring. This includes estimates of bond energies, entropies and heat capacities of radical

intermediates in pathways to chlorodioxin formation. Literature data for benzenes substituted with chlorines, fluorines, hydroxys and methyls was used to estimate ortho, meta, para and non-next-nearest neighbor interactions between (Cl-Cl), (Cl-OH), (CH₃-CH₃), (Cl-OH-Cl), and (OH-OH) substituents. Buttress effect between three adjacent bulky groups, such as methyls, is incorporated by evaluating literature values from polymethyl benzenes. A scheme is proposed to count the number of effective interactions between substituent groups on the ring for polysubstituted aromatics. Group values for the ortho, meta, para and non-next-nearest neighbor interactions are presented, and calculations to predict the thermodynamic properties are illustrated. Predictions for enthalpy, entropy and heat capacities for multiply substituted aromatics using this technique and our interaction groups give values that are in good agreement with literature data. The properties demonstrate that it is thermodynamically more favorable to form chlorinated dioxins and dibenofurans (especially the 2,3,7,8 isomer) over the respective non-chlorinated species.

REACTION PATHWAYS LEADING TO THE FORMATION OF DIOXINS AND DIBENZOFURANS

Now that we have developed a method for estimating properties of molecules having significant non-next nearest neighbor contributions, we can use this to screen candidate radical precursors to chlorinated dibenzodioxin and dibenzofuran formation. In addition we may consider possible reaction paths to the formation of these species. Several such reaction paths and energy level diagrams are illustrated in the figures that follow.

Figure 1 shows an energy level diagram for the isomerization of a polychlorinated phenylphenoxy radical. This species may result from oxygen attack (addition to an unsaturated carbon ortho to the biphenyl linkage) on a chlorinated biphenyl with subsequent loss of H atom. The displacement reaction forming phenylphenoxy radical is more than 17 kcal/mol exothermic. The oxy radical can attack the second ring at a position of chlorine substitution resulting in the resonantly stabilized chlorinated dihydrodibenzofuran radical intermediate shown. The new carbon-oxygen bond formed is weaker by only about 3.5 kcal/mol than the carbon-chlorine bond which must break for reaction to dibenzofuran to occur. Since the entropy change for this chlorine displacement reaction is favorable, a significant fraction of the complexes can dissociate by loss of chlorine resulting in the stable hexachlorodibenzofuran. It is important to

note that it is significantly less endothermic to form hexachlorinated dibenzofuran than it is to form dibenzofuran from the analogous non-chlorinated phenylphenoxy radical. Thermodynamic properties for species involved in this reaction, as well as other species in this work are estimated using the THERM computer code(5). THERM incorporates our interaction groups along with the group additivity method. Bond energies used for the estimation of radical properties can be calculated from the energy level diagrams illustrated. Here, for example each chlorine substitution on the ring reduces, the respective C-Cl or C-H bond energy by 1 kcal/mol. Bond energies used for estimation of these resonance stabilized intermediates account for stabilization by substituents on the rings, as well as resonance stabilization as shown by Herndon and Stein⁽³⁹⁾ and Stein and Golden⁽⁴⁰⁾. We have found that formula # 20 in reference (39) accurately predicts stabilization energies for conjugated allylic and benzylic systems when the radical is not in the cyclic or ring system. Formula # 3 in reference (40) accurately predicts stabilization for cyclic structures when the radical is in the ring system. Thermodynamic analysis of the overall reaction represented by figure 1 using THERM(5) indicates that the reaction is entropy driven, i.e., ΔG is negative, despite the reaction being endothermic. For temperatures above 300 K, a thermodynamic analysis for the overall reaction of hexachlorophenylphenoxy to hexachlorodibenzofuran plus chlorine atoms is

represented in Table XIII. As temperature increases the change in Gibbs Free Energy becomes more negative indicating that equilibrium favors products over reactants.

Figure 2 presents an energy level diagram for oxygen atom addition to trichlorodiphenylether at a position ortho to the ether linkage. This illustrates a plausible route to a phenoxyphenylether radical similar to the initial radical shown in Figure 1. Here, an ether linkage replaces biphenyl. In contrast to the previous example, the carbon-oxygen bond which is formed is nearly 17 kcal/mol stronger than the carbon-hydrogen bond which must break for reaction products to occur. The energized complex would be expected to rapidly lose H atom resulting in the chlorinated phenoxy diphenylether radical product at pressures up to 10 atmospheres with little stabilization. Further reaction of the product with itself, similar to reaction in Figure 1, may result in trichlorodibenzodioxin, but the energetics of this isomerization are not as favorable as those for the previous example (Figure 1). A thermodynamic analysis of the overall displacement reaction shown in Figure 2 indicates that Gibbs Free Energy has a minimum near 1100 K. This means that equilibrium favors products more at this temperature than higher or lower temperatures.

Figure 3 presents a potential energy diagram showing the isomerization of heptachlorinated phenoxyphenylether radical. Since it is not possible to accurately assign a degree of aromaticity to the intermediate radical, the well is drawn with two wells to bracket the Hf (300 K) of the

radical adduct. The higher Hf considers interactions between the oxygen in the plane of the radical and the chlorines on the cyclohexadiene radical, in addition to the interaction between chlorine on the fully aromatic ring and oxygen. The smaller Hf (11.6 kcal/mol lower) considers the above interactions as well as half the number of Cl-O interactions with the remaining oxygen. Only one half the aromatic interactions are counted since the oxygen being considered is not in the plane of the cyclohexadiene radical, but can flip back and forth spending some time in the plane of the radical. We feel these two values should bracket Hf for the radical adduct. Although the overall reaction is slightly endothermic, analysis of ΔG reaction indicates that the reaction is driven to the forward direction by entropy, with the equilibrium constant increasing with temperature. Reaction analysis of this overall reaction is represented in Table XIV for temperatures above 300 K.

Figure 4 illustrates an energy level diagram for reaction of molecular oxygen with a nonchlorinated phenylphenoxy radical. The intermediate peroxy radical can be collisionally stabilized into a shallow well of about 9 kcal/mol. This well depth is a conservative estimate based on bond energy of CF_3O-O_2 given by Francisco and Williams(18). The peroxy radical can lose HO_2 to give dibenzofuran. This is not an elementary reaction, but could occur on surfaces, or through further complex formation. A

thermodynamic analysis of this system shows that although the overall reaction is exothermic, entropy change is unfavorable, driving it in the reverse direction. The change in Gibbs Free Energy for overall reaction is negative indicating that products will be formed, unless stabilization occurs on the surface.

Formation of Dibenzodioxins

Figure 5 presents a potential energy diagram for oxygen atom addition at the C-C (phenyl-phenyl) linkage of a hexachlorinated dibenzofuran. The diradical formed is resonantly stabilized and can intraconvert between three isomeric forms. The most stable of these is a hexachlorinated phenoxy phenyl ether diradical which can undergo ring closure to form hexachlorinated dibenzodioxin. As in figure 3, Hf estimates have large uncertainties. As a result, two well depth values are shown bracketing the probable Hf for the diradical adducts. The thermodynamics of this system favor reaction to the dibenzodioxin product even at higher temperatures.

Formation of diphenyl ethers in reaction systems such as those in incinerators, where biphenyls and chlorobenzene are not present in the feed stream, may occur from reactions of phenoxy with benzene and other aromatic species. We note that calculations using groups developed here, predict that reaction of phenoxy with tetrachlorobenzene to yield trichlorodiphenylether plus Cl is exothermic by nearly 2 kcal/mol (as shown in Figure 6), with a small negative

entropy change. In contrast, the analogous reaction of benzene with phenoxy to give diphenylether plus H atom is endothermic by about 35 kcal/mol, with the entropy change for this reaction also unfavorable.

Phenoxy and substituted phenoxy radicals are easily produced from the reaction of benzene or substituted benzenes with oxygen atoms. Figure 7 shows a potential energy diagram of such a reaction. This is only one possible route to the formation of phenoxy radicals that may be of importance to dioxin formation. The energetics of these systems favor reaction to phenoxy plus H atom. Quantum Rice-Ramsperger-Kassel(22) (QRRK) calculations on the chemically activated reaction pathway indicate that the phenoxy and hydrogen products dominate at pressures of about 1 atmosphere and high temperatures. Another energetically favorable pathway to phenoxy radical is by the reaction of phenyl with O₂, as shown below:



Benzene may be formed from alkenes and alkynes through radical addition processes with subsequent ring closure. Westmoreland et. al. have shown a number of pathways to formation of benzene(23). We will now focus on an analogous route to the formation of pentachlorobezene as illustrated in Figure 8. Although the overall reaction of 1- chlorobutadiene radical and 1-chloroacetylene to yield chlorobenzene plus chlorine is exothermic; reaction analysis (ΔG) on

this overall reaction indicates that Gibbs Free Energy becomes less negative, i.e., less favorable with increasing temperature. For temperatures above 300 K a thermodynamic analysis for this overall reaction is shown in Table XV. Figure 9 shows the thermodynamic data output as given by THERM for some of the species represented in Figures 1 to 8.

Formation of Dibenzodioxins and Dibenzofurans in Incinerators and oxidative pyrolysis reactors

Using thermodynamics and reaction paths described in this thesis, one may visualize several regimes in an incinerator or pyrolysis reactor where chlorinated dibenzodioxins may be formed. One of these regimes is the fuel rich zone where hydrocarbons or fuel are fed to the reactor and where mixing is not complete. Temperatures in this region are high enough for pyrolysis reactions to occur and molecular growth forms the aromatic and poly-aromatic and poly-phenyl systems⁽²³⁻²⁵⁾. In addition, there is a significant amount, but not an excess, of oxygen and oxy radicals present to react with some of these aromatic compounds.

The reaction paths presented here demonstrate that dioxin and dibenzofuran formation from chlorinated ring systems are more favorable than formation from the analogous non-chlorinated systems. We wish to further point out that this reaction regime is very complex with rapid growth and dissociation occurring for many of the addition reaction systems and studies on these systems with hydrocarbons

show that there is only a low steady state concentration of these small ring compounds which are needed for formation of dioxins and dibenzofurans. Rapid molecular weight growth may, therefore, be a significant benefit to limiting formations of dibenzodioxins because it may rapidly deplete the pool of one to three ring systems needed for their formation. On the other hand, we may find as our analytical capabilities continue to increase that much higher molecular weight compounds in these series are formed and present even more risk to our environment. We know of no environmental studies on dioxin exposures that clearly present any indication of this however.

A second regime where dibenzodioxins and/or dibenzofurans may be formed is where benzene, biphenyl, terphenyls, etc. are present with oxygen and oxy radicals at lower temperatures (where oxidation reactions are slow and addition reactions are favored). This could occur at inlet conditions for feeds of these species, within the incinerator or kiln itself where poor mixing occurs, or at the outlet where these species formed in the combustor have not been converted to CO_2 and H_2O . The addition and displacement reactions discussed in this thesis would readily occur in cool down sections of reactor exhaust zones, for example.

We note that oxygenated radical species such as NO_3 , SO_3 and HO_2 may also add to the unsaturated ring systems in this regime. Subsequently, homogeneous and heterogeneous reactions, for example with HO_2 , could cleave the weaker

peroxy O-O bond and might also lead to dioxin formation. We are continuing work on plausible thermodynamic pathways for these types of reactions in addition to development of reaction mechanisms (series of elementary reactions) to predict levels of chlorinated dioxins in gas phase systems.

Results

Analyses on the pathways presented demonstrate plausible elementary reactions leading to chlorinated dibenzofuran and dioxin formation in incineration and combustion systems. Reaction paths are also presented to the formation of chlorinated aromatics from non-cyclic precursors. The initial presence of chlorinated aromatics and/or biphenyls is not required for dioxin formation, because these species can be readily formed through the reactions of chlorinated hydrocarbons.

A reaction pathway is also presented which shows the formation of chlorobenzene from chloroalkenes, a possible route to the formation of chlorodioxins starting with chlorinated alkanes. Thermodynamic analysis is carried out for each of these reaction pathways at temperatures representative of incineration conditions, demonstrating negative Gibbs Free Energies.

We suggest two plausible regimes where homogeneous dibenzo dioxin formation may occur. The first is the fuelrich (primarily pyrolysis) region where molecular weight growth may occur. Second is a region where polyphenyls and aro-

matics may be present with oxygen and oxy radicals at temperatures which favor addition reactions over oxidation of the ring systems. These regimes are very complex and previous studies indicate that dioxin precursors are present at very low steady state levels. Rapid molecular weight growth reactions appear capable of both forming and destroying the above mentioned precursors to dioxin.

QUANTUM RICE-RAMSPERGER-KASSEL (QRRK) ANALYSIS OF REACTION PATHWAYS

Introduction

Dibenzo-p-dioxins (Dioxin) and Dibenzofurans (DBF) are two classes of compounds which are thought to be highly toxic in nature. They are produced from a variety of sources such as automobile engines⁽²⁷⁾, combustion of aromatics⁽²⁸⁾, chlorophenol manufacture⁽²⁹⁾, etc. The presence of these compounds, even in very small amounts, is important because some of the chlorinated compounds are toxic at very low concentrations.

In order to predict the amount of dioxin formed during incineration processes, a detailed mechanism that can explain the formation from a variety of sources may be of significant value. Westmoreland et. al., (22) have illustrated a few reaction pathways which can lead to the formation of one ring aromatics during the pyrolysis and oxidation of one to three carbon hydrocarbons. Given a facile route to formation of aromatics from these small hydrocarbons, a reasonable starting point for the prediction of dioxin formation might be with the reactions and oxidation of aromatics. This would not only explain the formation of dioxins during oxidation of aromatics, but in conjunction with the known formation from lower molecular weight hydrocarbons, provide pathways which might explain

the homogeneous phase formation of dioxins starting from smaller hydrocarbons.

In order to develop an accurate mechanism for the prediction of dioxin formation during the oxidation of aromatics, a thermodynamic data base which contains properties such as: enthalpy, entropy and heat capacities of stable molecules and likely candidate radical precursors is required. Shaub^(16,17) realized the need for thermodynamic data and has developed a method to predict the enthalpies of formation for substituted aromatics and dioxins. We have improved Shaub's estimation technique for enthalpies, in addition to developing ring substituent terms (groups) which are used with Benson's group additivity method^(1,3). These terms predict: enthalpy, entropy and heat capacities of multisubstituted aromatics. The numerical computation (summing of individual groups and ring correction terms) is carried out by a computer code THERM⁽⁵⁾.

Experimental determination of dioxins and DBF in product/effluent streams show that chlorinated dioxin and DBF are produced in larger amounts than the corresponding non chlorinated ones⁽²⁸⁾. To explain this difference, each reaction which is proposed in this study will be analysed with and without chlorine on the reactants. Energized complex/QRRK theory for bimolecular reaction as described by Dean⁽³⁰⁾ and by Westmoreland et. al.,⁽³¹⁾ is used to model reactions between: atoms or radicals with unsaturated molecules (addition to unsaturated bonds).

These kinetic calculations utilize the quantum RRK (QRRK) reaction theory of Kassel⁽³²⁾, which treats the storage of excess energy as quantized vibrational energy. The bimolecular case utilized here incorporates recombination or addition to form the energized complex followed by stabilization, reaction to products or dissociation back to reactants. The algorithm presented by Dean⁽³⁰⁾ was modified to include Gamma function evaluation of reaction probability as a function of energy and the chemical activation distribution function, to replace the factorials. Barriers (E_a/h) are not rounded to the nearest integer before summation with respect to energy, although the integer step for total energy is retained. This is expected to give more accurate estimates at lower temperatures, where small changes in barrier height may have significant effects.

Input data requirements are as follows:

- a: pre-exponential factors (Arrhenius A factors) in the high pressure limits, which are obtained from the literature and the methods of Benson⁽³⁾
- b: energies of activation come from heats of formation ΔH_f (298 K) for the involved species and from analogy to similar reactions with known energetics.
- c: number of vibrational degrees of freedom
- d: geometric mean vibrational frequency of the adduct comes from computer code CPFIT developed by Ritter⁽⁵⁾ .
- e: Lennard-Jones transport properties e/k and are estimated if not available in literature. e/k values

for chlorinated species are estimated by taking the difference between chlorobenzene and benzene, and then adding this difference for each chlorine substitution to ρ/k of the non chlorinated parent molecule. Values for chlorinated species are estimated by taking the difference (Δ) between chlorobenzene and benzene. In case of para substitution, or biphenyl and diphenyl ethers two of the above mentioned differences (Δ) are added to the parent molecule. In all other cases only one difference (Δ) is added to the parent property.

A collision efficiency, Beta β , is applied to modify the strong collision assumption so that $k(\text{deactivation}) = \beta Z[M]$, where Z is the collision frequency. Beta is calculated from the fit of Troe⁽³³⁾, with average energy transferred per collision (ΔE_{coll}) from comparison to compilations by Troe^(34,35) and by Gardiner and Troe⁽³⁶⁾. The third body or bath gas is taken to be air.

REACTION OF CHLOROBENZENE WITH OXYGEN ATOM

The first reaction we shall discuss is the addition of oxygen atom to chlorobenzene to form the chlorophenoxy adduct. This adduct can either dissociate back to reactants, be stabilized, or dissociate to chlorophenoxy and hydrogen as products. The corresponding reaction in the non chlorinated system involves addition of oxygen atom to benzene, formation of phenoxy adduct, and dissociation of this adduct either back to reactants, or to phenoxy and

hydrogen products. For the chlorinated system the reaction is slightly more exothermic than the corresponding reaction of oxygen atom with benzene (-16.84 vs -15.84 kcal/mol at 298 K), and a reaction analysis of the overall reaction indicates that Gibbs Free Energy for reaction without chlorines is slightly more negative than the reaction with chlorines (-15.74 vs -15.37 kcal/mol at 300 K). The reaction with chlorines is therefore slightly more favorable than the one without chlorines. QRRK analysis is not carried out for this system because the reactions have fairly large negative ΔH and ΔG values, and all reaction to the complex will go to products.

REACTION OF PHENOXY WITH 1,2,3,5-TETRACHLOROBENZENE

Figure 6 shows the energy level diagram for the reaction of phenoxy radical with 1,2,3,5-tetrachloro benzene. The ether complex which is formed can dissociate back to reactants, be stabilized by collisions or dissociate to Cl and 1,2,3-trichlorobiphenyl ether products. The corresponding reaction of the non chlorinated species is addition of a phenoxy radical to benzene, with H and biphenyl ether as the products for this reaction. The reaction with tetrachloro benzene at 298 K is slightly exothermic, ΔH_f of -1.7 kcal/mol, while the reaction with benzene is endothermic with a ΔH_f of 33.37 kcal/mol, i.e., the reaction involving chlorobenzene is 35 kcal/mol more

exothermic. The entropy changes for the tetra chlorinated benzene and benzene reactions at 298 K are -10.63 cal/mol-K and -7.810 cal/mol-K respectively. Gibb's Free Energy change for the chlorinated system at 300 K, 500 K and 1000 K are -1.34 kcal/mol, -1.04 kcal/mol and -0.9 kcal/mol respectively, while for the nonchlorinated system they are 35.7 kcal/mol, 37.1 kcal/mol and 39.2 kcal/mol clearly indicating that the chlorinated version of the reaction is significantly more thermodynamically favored than the non chlorinated one.

A QRRK analysis is carried out for the reaction shown in Figure 6, with input parameters and references listed in Table XVI. Results from the analysis are shown in graphs G1-A to G1-C. Graph G1-A is a plot of $\log(k_1)$ (reactant going to stabilized complex, $\text{cm}^3 \text{s}^{-1} \text{mol}^{-1}$) vs., $1000/T$ for pressures ranging from 0.01 to 500 atm. This rate constant increases with increase in pressure, and gradually decreases with increase in temperature, indicating that high pressures and lower temperatures are favorable to the formation of the ether. Graph G1-B is a plot of $\log(k_2)$ (reactants going to products via energized complex, s^{-1}) vs., $1000/T$ for pressure ranging from 0.01 atm to 500 atm. This graph shows that the rate constant (k_2) decreases slightly with pressure, and increases with increasing temperature. Graph G1-C is a plot of $\log(k_{-1})$ (energized complex dissociating back to reactants, s^{-1}) vs., $1000/T$ for pressures from 0.01 to 500 atm. This rate constant

decreases with increasing pressure, and increases with temperature.

At typical incinerator operating conditions (1100 K and 1 atm pressure) the ratio of k_2/k_1 is 262 mol/cm³ and k_2/k_{-1} is 0.4. Graphs G1-A to G1-C indicates that almost no stabilization takes place, and that the energized complex dissociating to products accounts for about 40 % of the reaction. Graph G1-C indicates that the remaining 60 % of the energized complex dissociates back to reactants. At typical stack conditions (500 K and 1 atm pressure) the ratio of k_2/k_1 is 6.9 while k_2/k_{-1} is 5.4. Thus, at these conditions Graph G1-A shows that stabilization accounts for about 11 % of the energized complex, while dissociation to products shown in Graph G1-B accounts for more than 75 %, the remaining dissociating back to reactants. Thus more trichlorophenyl ether will be formed in the cooler stack conditions than the hotter incinerator.

REACTION OF OXYGEN ATOM WITH HEPTACHLOROBIPHENYL

Figure 10 shows the energy level diagram for the reaction of oxygen atom with 1,2,3,5,2',3',4'heptachloro biphenyl. The complex formed can dissociate back to the reactants, stabilize, or dissociate to H and heptachlorophenyl phenoxy as products. The corresponding reaction without chlorines is between oxygen atom and biphenyl, giving H and biphenyl phenoxy as products. The heptachloro biphenyl reaction at 298 K has a ΔH_f of -25.07 kcal/mol

and a ΔS of -5.39 cal/mol-K, while the property changes for the biphenyl reaction at the same temperature are -15.15 kcal/mol and -0.95 cal/mol-K, respectively. Clearly both reactions take place due to the negative ΔG s, but the reaction of heptachloro biphenyl has a lower (more favorable) ΔG (-23.46 kcal/mol vs -14.86 kcal/mol at 298 K). At 500 and 1000 K the ΔG values for the chlorinated system are -27.73 kcal/mol and -28.92 kcal/mol respectively while for the nonchlorinated system they are -13.91 kcal/mol and -12.2 kcal/mol respectively. These ΔG values indicate that as temperature increases the chlorinated reaction becomes more favorable over the nonchlorinated reaction.

A QRRK analysis is carried out for the reaction in Figure 10, with input parameters and references given in Table XVII. Results from the analysis are shown in graphs G2-A to G2-C. Graph G2-A is a plot of $\log(k_1)$ (reactants going to stabilized complex, $\text{cm}^3 \text{s}^{-1} \text{mol}^{-1}$) vs $1000/T$ from pressures of 0.01 to 500 atm. This rate constant is a function of pressure, and increases with increasing pressure. Graph G2-B is a plot of $\log(k_2)$ (reactants going to products via energized complex, s^{-1}) vs $1000/T$ for pressures ranging from 0.01 to 500 atm. This rate constant decreases slightly with pressure, and increases with increasing temperature. Graph G2-C is a plot of $\log(k_{-1})$ (energized complex giving reactants, s^{-1}) vs $1000/T$ for pressures ranging from 0.01 to 500 atm. This rate constant decreases slightly with pressure, and increases with increasing temperatures.

At typical incinerator conditions (1100 K and 1 atm pressure) the ratio k_2/k_1 is 360 mol/cm^3 , while k_2/k_{-1} is 4890. Graphs G2-A to G2-C indicate that all the reactants will be converted to products with no stabilization of the energized complex or its dissociation back to reactants. At 500 K and 1 atm the two above mentioned ratios become 31.4 mol/cm^3 and 16 E6 respectively. The graphs indicate that about 3 % of the energized complex will get stabilized while the rest goes to products. There is no dissociation of the energized complex back to reactants in this case. Although both stack and incinerator conditions are favorable for the reactants to go to products, the higher temperature (incinerator) is slightly more favorable as 100 % of the reactants get converted to products versus 97 % in the stack conditions.

ISOMERIZATION OF HEPTACHLOROBIPHENYL PHENOXY

An energy level for the isomerization of heptachlorophenyl phenoxy radical is shown in Figure 1. The complex formed can dissociate back to the parent radical, be stabilized by collisions, or dissociate to Cl and hexachlorodibenzofuran as products. The corresponding reaction without chlorines involves the isomerization of biphenyl phenoxy, giving dibenzofuran as products. At 300 K isomerization of heptachlorophenyl phenoxy although slightly endothermic ($\Delta H_f = 5.79 \text{ kcal/mol}$) has a sufficiently large entropy change ($\Delta S = 22.5 \text{ cal/mol-k}$) to give a small negative

Gibbs Free Energy change ($\Delta G = -0.92$ kcal/mol). The isomerization of phenyl phenoxy at 300 K is endothermic ($\Delta H_f = 33.14$ kcal/mol) and has a large negative entropy change ($\Delta S = -12.05$ cal/mol-k) giving a very unfavorable change in Gibbs Free Energy ($\Delta G = 36.73$ kcal/mol). At 500 K and 1000 K the ΔG values for chlorinated system are -5.23 kcal/mol and -15.28 kcal/mol respectively, while those for nonchlorinated system are 28.39 kcal/mol and 19.85 kcal/mol respectively. These ΔG values clearly indicates that reaction of the chlorinated system is far more favorable than the corresponding non chlorinated reaction.

A QRRK analysis is carried out for the reaction represented in Figure 1, with the input parameters and references listed in Table XVIII. Results from the analysis are shown in Graphs G3-A to G3-C. Graph G3-A is a plot of $\log(k_1)$ (reactant giving stabilized complex, $\text{cm}^3 \text{s}^{-1} \text{mol}^{-1}$) vs $1000/T$ for pressures from 0.01 to 500 atm. Graph G3-B is a plot of $\log(k_2)$ (reactant going to products via energized complex, s^{-1}) vs $1000/T$ for pressures ranging from 0.01 to 500 atm. Graph G3-C is a plot of $\log(k_{-1})$ (energized complex giving reactants, s^{-1}) vs $1000/T$ for pressure ranging from 0.01 to 500 atm.

At typical incinerator conditions (1100 K and 1 atm pressure) the ratio of k_2/k_1 is 1 mol/cm^3 and k_2/k_{-1} is 9. Graphs G3-A to G3-C indicate that all the three paths are important. Dissociation of the energized complex back to reactants shown in graph G3-C account for about 5.3 % of

the energized complex formed, while the remaining is divided equally between dissociation to products and stabilization. At typical stack conditions (500 K and 1 atm pressure), the above two ratios are 0.0065 mol/cm³ and 17.5, respectively, and the data shows that all the energized complex formed stabilizes, with no dissociation to products or reactants. Thus, for the reactants to go to products, the higher temperature (incinerator) conditions are necessary.

REACTION OF OXYGEN ATOM WITH TRICHLOROBIPHENYL ETHER

Figure 11 shows the energy level diagram for the reaction of oxygen with 1,2,3-trichlorobiphenyl ether. The adduct formed can dissociate back to the reactants, or be stabilized, or form H and 1,2,3-trichlorophenyl phenoxy ether as products. The corresponding reaction without chlorines involves attack of oxygen atom on biphenyl ether, giving H and phenyl phenoxy ether as products. The reaction of trichlorobiphenyl ether at 298 K is more exothermic than the reaction of biphenyl ether (-28.23 kcal/mol vs -17.29 kcal/mol) with a slightly more negative entropy change (-5.42 cal/mol-K vs -4.15 cal/mol-K). Although at 300 K both reactions have negative Gibb's Free Energy (-26.58 kcal/mol and -16 kcal/mol), the trichlorobiphenyl ether reaction has a larger negative value. At temperatures of 500 K and 1000 K the ΔG values for the chlorinated system are -25.69 kcal/mol and -24.22 kcal/mol, while for the

nonchlorinated system they are -13.3 kcal/mol and -12.93 kcal/mol respectively, indicating that even at high temperature the chlorinated reaction has a higher (more negative) ΔG change than for the nonchlorinated reaction.

A QRRK analysis is carried out for the reaction represented in figure 11, with the input parameters and references listed in Table XVIII. Results from the analysis are shown in graphs G4-A to G4-C. Graph G4-A is a plot of $\log(k_1)$ (reactant going to stabilized complex, $\text{cm}^3 \text{s}^{-1} \text{mol}^{-1}$) vs $1000/T$ for pressures from 0.01 to 500 atm. Graph G4-B is a plot of $\log(k_2)$ (reactants going to products via energized complex, s^{-1}) vs $1000/T$ for pressures ranging from 0.01 to 500 atm. Graph G4-C is a plot of $\log(k_{-1})$ (energized complex giving reactants, s^{-1}) vs $1000/T$ for pressures ranging from 0.01 to 500 atm.

At typical incinerator conditions (1100 K and 1 atm pressure) the ratio of k_2/k_1 is 116 mol/cm^3 and k_2/k_{-1} is 59. Data from the graphs indicate that about 1.6 % of the energized complex dissociates back to reactants, while the remaining dissociates to products with negligible stabilization (0.85 %). At typical stack conditions (500 K and 1 atm pressure) the ratios are 8.2 mol/cm^3 and 45000, respectively, and the data from the graphs indicate that now about 11 % of the energized complex stabilizes while the remaining 89 % goes to products with no dissociation of the energized complex forming reactants. Thus both low and high temperature conditions give more than 89 % of

reactants going to products, but the higher temperature (incinerator) conditions show more products will be formed.

ISOMERIZATION OF HEPTACHLOROPHENYL PHENOXY ETHER

Figure 3 shows the energy level diagram for the isomerization of the heptachlorophenyl phenoxy ether radical. The complex formed can dissociate back to the parent radical, be stabilized, or form Cl and 1,2,3,5,6,7-hexachlorodibenzo-p-dioxin as products. The corresponding reaction without chlorines involves isomerization of phenyl phenoxy ether radical giving dibenzo-p-dioxin. Although the isomerization of heptachlorophenyl phenoxy at 298 K is slightly endothermic ($\Delta H = 0.88$ kcal/mol) the entropy change is sufficiently large ($\Delta S = 15.1$ cal/mol-K) for the process to have a favorable Gibbs Free Energy change ($\Delta G = -3.62$ kcal/mol). The isomerization of phenyl phenoxy radical at 298 K is slightly more endothermic ($\Delta H = 8.84$ kcal/mol), with a larger entropy change ($\Delta S = 25.01$ cal/mol-k). This yields a less favorable Gibbs Free Energy change ($\Delta G = 1.38$ kcal/mol). At temperatures of 500 K and 1000 K the ΔG values for the chlorinated system are -6.5 kcal/mol and -13.21 kcal/mol respectively, while for the nonchlorinated system they are -1.2 kcal/mol and -7.89 kcal/mol. ΔG values for the chlorinated system are more negative than the corresponding values for the nonchlorinated system, clearly indicating that the chlorinated system is much more favorable over the non chlorinated one.

A QRRK analysis is carried out for the reaction represented in Figure 3, with the input parameters and references listed in Table XX. Results from the analysis are shown in graphs G5-A to G5-C. Graph G5-A is a plot of $\log(k_1)$ (reactants going to stabilized complex, $\text{cm}^3 \text{s}^{-1} \text{mol}^{-1}$) vs $1000/T$ for pressures from 0.01 to 500 atm. Graph G5-B is a plot of $\log(k_2)$ (reactant going to products via energized complex, s^{-1}) for pressures ranging from 0.01 to 500 atm. Graph G5-C is a plot of $\log(k_{-1})$ (energized complex going to reactants, s^{-1}) vs $1000/T$ for pressures ranging from 0.01 to 500 atm.

At typical incinerator conditions (1100 K and 1 atm pressure) the ratio of k_2/k_1 is 2.5 mol/cm^3 and k_2/k_{-1} is 1.8. Data from the graphs indicate that all three channels are important, and that 50.7 % of the energized complex goes to products, while 29 % of it dissociates back to reactants and the remaining 20.3 % stabilizing. At typical stack conditions (500 K and 1 atm pressure) the above ratios are 0.0014 mol/cm^3 and 8.3 respectively indicating that all the energized complex formed will get stabilized, and there is no dissociation of the energized complex to products or reactants. Thus for the reactants to go to products the hot incinerator conditions are necessary, and that no products will be formed in the stack from this reaction.

Results

From the above QRRK analysis we observe that in all but one case the higher temperature (incinerator) conditions of 1100 K and 1 atm pressure give more conversion of reactants to products. In the reaction of phenoxy with 1,2,3,5-tetrachloro benzene where stack conditions are more favorable (500 K and 1 atm pressure) significant amount of products are formed (40 %) even at the hotter incinerator conditions. Thus, from this we can conclude, that based on the reaction pathways presented in this study, the hotter incinerator conditions can lead to significant amount of vapor phase dioxins. We also conclude from the comparision of the reaction pathways for chlorinated systems versus similar pathways for non chlorinated systems, that the levels of chlorinated dioxins formed will be greater than the non chlorinated one.

APPENDIX A

RING CORRECTION GROUPS

TABLE I
Ring corrections for hydrocarbons

RING	H ₂₉₈	S ₂₉₈	CP ₃₀₀	CP ₄₀₀	CP ₅₀₀	CP ₆₀₀	CP ₈₀₀	CP ₁₀₀₀
cyC3	27.53	32.04	-3.13	-2.67	-2.32	-2.11	-1.92	-1.84
cyC3 1e	53.34	33.43	-0.32	-0.62	-0.78	-0.93	-1.27	-1.52
cyC4	26.51	29.88	-5.02	-4.46	-3.83	-3.31	-2.57	-2.12
cyC4 1e	29.79	28.45	-3.05	-2.73	-2.30	-1.97	-1.64	-1.43
cyC5	5.91	22.90 ^a	-7.57	-6.51	-5.39	-4.43	-3.06	-2.22
cyC5 1e	5.09	25.22	-4.50	-3.94	-3.29	-2.76	-2.08	-1.63
cyC5 2e	4.81	27.97	-3.80	-3.75	-3.30	-2.78	-2.09	-1.94
cyC6	0.00	18.38	-7.64	-6.17	-4.40	-2.72	-0.20	1.11
cyC6 1e	1.10	21.21	-5.14	-4.29	-3.35	-2.54	-1.41	-0.66
cyC6 2e-14	0.27	21.28	-3.14	-3.19	-2.54	-1.95	-1.19	-0.76
cyC6 2e-13	4.19	25.57	-4.82	-4.46	-4.00	-3.26	-2.17	-1.64
cyC7	6.26	17.26 ^b	-6.73	-4.86	-3.14	-1.17	0.06	1.07
cyC7 1e	4.88	15.55	-5.21	-4.17	-3.10	-2.16	-0.84	0.03
cyC7 2e-13	6.22	22.28	-4.68	-4.79	-3.89	-3.09	-1.81	-1.15
cyC7 3e	3.68	23.92	-5.30	-5.89	-5.50	-4.68	-3.24	-2.71

cyC8	9.71	12.31	-8.82	-7.28	-5.52	-3.90	-1.45	0.10
c cyC8	5.61	12.10	-6.17	-4.51	-2.93	-1.65	0.04	1.06
1e d cyC8	7.88	20.13	-5.09	-4.67	-3.78	-2.79	-1.28	-0.47
2e-13 d cyC8	-1.32	14.07	-3.84	-2.62	-1.32	-0.25	1.05	1.76
2e-15 cyC8								
4e	16.89	29.82	-6.20	-7.64	-7.53	-6.55	-4.51	-3.94
a	VALUE FOR = 1 (4), 27.53 FOR = 10 (3)							
b	VALUE FOR = 2 (4), 15.95 FOR = 1 (3)							
c	TRANS							
d	CIS, CIS							

TABLE II
Ring correction for saturated hydrocarbons with oxygen

RING	H ₂₉₈	S ₂₉₈	CP ₃₀₀	CP ₄₀₀	CP ₅₀₀	CP ₆₀₀	CP ₈₀₀	CP ₁₀₀₀
CyC20	26.82	29.22	-1.80	-2.09	-2.24	-2.31	-2.22	-1.90
CyC30	25.97	27.15	-3.36	-3.50	-3.50	-3.19	-2.33	-1.66
CyC40	5.63	26.76	-5.25	-5.12	-4.86	-4.39	-3.25	-2.21
CyC50	-0.51	15.31	-4.55	-3.89	-3.26	-1.93	0.65	1.90
CyC60	5.73	14.64	-5.45	-4.40	-3.45	-2.31	-0.31	0.87
CyC70	9.17	12.04	-7.54	-6.70	-5.82	-4.48	-1.82	-0.09
a CyC4 _p02	3.30	16.47	-4.16		-3.11		-1.09	-0.47

a calculated from the data from Stull et al⁽⁶⁾

TABLE III
Ring corrections for unsaturated hydrocarbons with oxygen

RING	H ₂₉₈	S ₂₉₈	CP ₃₀₀	CP ₅₀₀	CP ₈₀₀	CP ₁₀₀₀
cyC40 1e	-2.26	26.38	-4.16	-3.49	-2.23	-1.68
^a cyC40 2e	-6.05	25.00	-4.97	-3.07	-1.89	-1.73
cyC50 1e-1	-5.79	17.12	-4.80	-3.54	-1.56	-0.70
cyC50 2e-14	-14.04	18.31	-4.57	-2.32	-0.96	0.59
cyC50 2e-13	-14.04	22.44	-4.57	-2.32	-0.96	-0.64

a calculated from data in Stull⁽⁶⁾

TABLE IV
Ring corrections for saturated hydrocarbons with nitrogen

RING	H ₂₉₈	S ₂₉₈	CP ₃₀₀	CP ₄₀₀	CP ₅₀₀	CP ₆₀₀	CP ₈₀₀	CP ₁₀₀₀
^a cyC2N	27.50	28.99	-2.33	-2.24	-2.13	-2.01	-1.78	-1.57
^b cyC3N	26.20	39.30	-3.89	-3.52	-3.17	-2.73	-1.89	-1.33
cyC4N	6.80	26.70	-6.17	-5.44	-4.80	-4.08	-2.87	-2.17
cyC5N	1.00	15.74	-5.08	-3.92	-2.93	-1.47	1.09	2.23
cyC6N	6.95	16.45	-5.97	-4.36	-3.12	-1.66	0.53	1.18
cyC7N	10.39	14.25	-8.07	-6.72	-5.49	-4.01	-1.38	0.24

a estimated from the data in Stull⁽⁶⁾

b from Benson⁽³⁾

TABLE V
Ring corrections for unsaturated hydrocarbons with nitrogen

RING	H ₂₉₈	S ₂₉₈	CP ₃₀₀	CP ₄₀₀	CP ₅₀₀	CP ₆₀₀	CP ₈₀₀	CP ₁₀₀₀
cyC4N 1e-1	11.85	27.27	-6.19	-5.97	-4.36	-3.12	-1.66	0.53
cyC5N 1e-1	1.00	15.74	-5.08	-3.92	-2.93	-1.47	1.09	2.23

TABLE VI
Ring corrections for saturated hydrocarbons with sulfur

RING	H ₂₉₈	S ₂₉₈	CP ₃₀₀	CP ₅₀₀	CP ₈₀₀	CP ₁₀₀₀
cyC2S	19.44	29.48	-2.85	-2.66	-4.32	-5.82
cyC3S	19.33	27.22	-4.59	-3.91	-4.60	-5.70
cyC4S	1.50	23.56	-4.90	-3.65	-4.41	-5.57
cyC5S	-0.54	16.09	-6.22	-2.24	0.86	1.29
cyC6S	4.85	15.91	-7.75	-1.22	4.79	4.61
cyC7S	9.67	12.54	-9.25	-5.96	-1.22	0.80

TABLE VII
Ring corrections for unsaturated hydrocarbons with sulfur

RING	H ₂₉₈	S ₂₉₈	CP ₃₀₀	CP ₅₀₀	CP ₈₀₀	CP ₁₀₀₀
cyC3S 1e-1	17.78	25.20	-2.97	-2.76	-6.16	-7.32
cyC4S 1e-1	a 1.92	24.58	-2.13	-1.68	-4.62	-7.03
cyC4S 1e-2	a 4.16	29.31	-1.91	-2.19	-6.03	-5.52
cyC4S 2e	b -16.52	22.79	-4.51	-3.18	-3.93	-5.31
cyC5S 1e-1	-4.95	17.09	-4.02	-1.27	-1.53	-2.52
cyC5S 2e-14	-20.69	19.26	-4.73	-4.33	-4.43	-5.57
cyC5S 2e-13	-19.10	21.25	-5.03	-4.62	-6.59	-7.34

a Enthalpy of formation data from Pedley⁽⁷⁾
b Thermodynamic data from Stull⁽⁶⁾

APPENDIX B

GROUP INTERACTION TERMS FOR AROMATIC RINGS AND
PREDICTED VALUES

Table VIII

Group values and group interactions used

Group	H	S	C _{P300}	C _{P500}	C _{P800}	C _{P1000}	C _{P1500}
C/C2/H2 ¹	-5.01	9.42	5.5	8.25	11.07	12.34	14.2
CB/H	3.3	11.5	3.28	5.46	7.51	8.31	9.68
CB/Cl ²	-4.11	18.55	7.17	9.16	10.34	10.68	9.66
CB/O ³	-1.63	-10.04	4.2	6.54	7.07	7.09	6.96
(Cl-Cl) ⁴ _{ORTHO}	2.18	-0.31	-0.2	-0.47	-0.44	0.38	1.01
(Cl-Cl) ⁴ _{META}	1.34	0.17	-0.12	-0.42	-0.43	-0.38	1.01
(Cl-Cl) ⁴ _{PARA}	0.52	-0.08	-0.1	-0.36	-0.37	-0.38	1.01
(F-F) ⁵ _{ORTHO}	5.13	0.2	-0.16	-0.67	-0.48	-0.8	1.31
(F-F) ⁵ _{META}	1.48	-0.17	-0.22	-0.77	-0.93	-1.06	0.81
(F-F) ⁵ _{PARA}	2.09	0.06	-0.16	-0.68	-0.92	-1.01	0.84
(CH ₃ -CH ₃) ⁶ _{ORTHO}	0.44	-1.05	1.82	-0.09	-1.52	-2.13	0.15
(CH ₃ -CH ₃) ⁶ _{META}	0.02	0.13	0.46	-0.77	-1.75	-2.25	0.07
(CH ₃ -CH ₃) ⁶ _{PARA}	0.19	0.25	0.29	-1.14	-2.02	-2.46	-0.06
(CH ₃ -OH) ⁷ _{ORTHO}	0.14	-0.06	1.15	0.05	-0.62	0.17	1.59
(CH ₃ -OH) ⁷ _{META}	-0.75	-0.26	-0.25	-0.66	-0.9	-0.15	1.39
(CH ₃ -OH) ⁷ _{PARA}	0.91	-1.06	-0.25	-0.79	-1.06	-0.25	1.33
(Cl-OH) ⁸ _{ORTHO}	4.53						
(Cl-OH) ⁸ _{META}	-6.26						
(Cl-OH) ⁸ _{PARA}	-4.46						
(Cl-OH-Cl) ⁹	13.85						

1 value suggested by Cohen⁽¹⁸⁾2 group evaluated using chlorobenzene data from Stull et al⁽¹⁶⁾3 group evaluated using phenol data from Stull et al⁽¹⁶⁾4 group evaluated using dichlorobenzene data from Stull et al⁽¹⁶⁾5 group evaluated using difluorobenzene data from Stull et al⁽¹⁶⁾6 group evaluated using xylene data from Stull et al⁽¹⁶⁾7 group evaluated using cresol data from Stull et al⁽¹⁶⁾8 group evaluated using chlorophenol data from Cox et al⁽²⁰⁾9 group evaluated using 1,4 dihydroxy 2,6 dichlorophenol data from Cox et al⁽²⁰⁾

Table IX

Comparison of enthalpy of formation in kcal/mol at 298K

Species	H _{f(lit)}	Source	H _f [*]	Deviation	H _f ^{**}	Deviation
1,2,3,4-tetra methylbenzene	-8.61	18	-9.04	0.43	-10.45	1.84
Penta methylbenzene	-14.92	18	-15.63	0.71	-17.87	2.95
Hexa methylbenzene	-18.79	18	-20.75	1.96	-24.72	5.93
Hexa chlorobenzene	-8.1	16	-7.04	-1.06	-9.6	1.5
Hexa fluorobenzene	-228.49	16	-228.85	0.36	-226.8	-1.69
Penta chlorophenol	-53.9	19	-52.63	-1.27	-49	-4.9
2,6-dimethylphenol	-38.64	10	-38.43	0.21	-37.14	-1.5
ortho cresol	-30.7	5	-30.74	0.04	-29.72	-0.98
meta cresol	-31.59	5	-31.63	0.04	-30.29	-1.3
para cresol	-29.94	5	-29.97	0.03	-30.29	0.35

Table X
Comparison of entropy in cal/mol-K at 298K

Species	$S_{f(lit)}$	Source	S_f^*	Deviation	S_f^{**}	Deviation
1,2,3,4-tetra methylbenzene	100.76	18	100.29	0.47	99	1.76
Penta methylbenzene	108.24	18	108.6	-0.36	106.4	1.84
Hexa methylbenzene	112	18	112.56	-0.56	108.62	3.54
Hexa chlorobenzene	105.45	16	106.31	-0.86	108.46	-3.01
Hexa fluorobenzene	91.35	16	91.57	-0.22	91.66	-0.31
ortho cresol	84.2	5	85.44	-1.24	84.72	-0.52
meta cresol	85.03	5	8.24	-0.21	86.33	-1.3
para cresol	83.77	5	83.06	0.71	84.95	-1.18

Table XI
Comparison of specific heats in cal/mol-K at 300K

Species	$C_{p(lit)}$	Source	C_p^*	Deviation	C_p^{**}	Deviation
1,2,3,4-tetramethylbenzene	44.69	18	44.88	-0.19	45.28	- 0.59
pentamethylbenzene	51.83	18	51	0.83	52.02	-0.19
hexamethylbenzene	57.98	18	58.55	-0.57	59.88	-1.9
hexachlorobenzene	43.02	16	41.36	0.67	44.4	-2.37
hexafluorobenzene	36.71	8	36.24	0.47	37.8	-1.09
ortho cresol	30.57	5	31.31	-0.74	28.14	2.43
meta cresol	29.95	5	29.91	0.04	27.02	2.93
para cresol	30.02	5	29.91	0.11	27.02	3.0

Table XII
Comparison of specific heats in cal/mol-K at 500K

Species	$C_{p(lit)}$	Source	C_p^*	Deviation	C_p^{**}	Deviation
1,2,3,4-tetramethylbenzene	66.03	3	65.56	0.47	67.14	- 1.11
pentamethylbenzene	72.26	3	74.42	-2.16	76.06	-3.8
hexamethylbenzene	83.48	3	80.97	2.51	86.28	-2.8
hexachlorobenzene	52.53	1	50.52	2.01	55.2	-2.67
hexafluorobenzene	48.87	7	45.43	3.44	51	-2.13
ortho cresol	46.64	5	46.91	-0.27	47.22	-0.58
meta cresol	46.46	5	46.2	0.44	4.92	0.54
para cresol	46.33	5	46.07	0.26	45.92	0.41

* Value using the method developed in this work

** Value using Benson's groups

APPENDIX C

REACTION ANALYSIS OUTPUT

REACTION ANALYSIS for 298 K

REACTION ENTERED: $C_{12}H_2OCl_7 \rightarrow C_{12}H_2OCl_6 + Cl$
 overall reaction represented in Figure 1

Hf (kcal/mol) -15.910 -39.010 28.900
 S (cal/mol K) 151.580 134.610 39.500

del H of reaction = 5.800 kcal/mol
 del S/R of reaction = 11.339
 del G/RT of reaction = -1.548

Af/Ar = 1.264E+00

T (K)	delta H (kcal)	del S/R	(Af/Ar)	del G/RT
300.000	5.791E+00	1.133E+01	1.239E+00	-1.610E+00
500.000	5.063E+00	1.037E+01	2.851E-01	-5.271E+00
800.000	4.691E+00	1.005E+01	1.298E-01	-7.099E+00
1000.000	4.733E+00	1.007E+01	1.062E-01	-7.691E+00
1200.000	4.770E+00	1.009E+01	9.008E-01	-8.090E+00
1500.000	4.420E+00	9.964E+00	6.351E-02	-8.481E+00
2000.000	2.682E+00	9.464E+00	2.890E-02	-8.789E+00

Table XIII : Thermodynamic analysis for reaction in Figure 1

REACTION ANALYSIS for 298 K

REACTION ENTERED: $C_{12}H_2O_2Cl_7 \rightarrow C_{12}H_2O_2Cl_6 + Cl$
 overall reaction represented in Figure 3

Hf (kcal/mol) -63.130 -91.180 28.900
 S (cal/mol K) 160.540 136.140 39.500

del H of reaction = .850 kcal/mol
 del S/R of reaction = 7.599
 del G/RT of reaction = -6.165

Af/Ar = 3.005E-02

T (K)	delta H (kcal)	del S/R	(Af/Ar)	del G/RT
300.000	8.415E-01	7.586E+00	2.944E-02	-6.174E+00
500.000	2.782E-01	6.827E+00	8.274E-03	-6.547E+00
800.000	1.735E-01	6.728E+00	4.681E-03	-6.619E+00
1000.000	3.275E-01	6.813E+00	4.078E-03	-6.648E+00
1200.000	6.298E-01	6.950E+00	3.899E-03	-6.686E+00
1500.000	1.423E+00	7.244E+00	4.185E-03	-6.767E+00
2000.000	2.916E+00	7.684E+00	4.874E-03	-6.951E+00

Table XIV : Thermodynamic analysis for reaction in Figure 3

REACTION ANALYSIS for 298 K

REACTION ENTERED: $C_4HCl_4 + C_2Cl_2 \rightarrow cy(C_6HCl_5) + Cl$
 overall reaction represented in Figure 8

Hf (kcal/mol)	41.080	41.400	-5.330	28.900
S (cal/mol K)	97.460	65.420	101.940	39.500

del H of reaction = -58.910 kcal/mol
 del S/R of reaction = -10.790
 del G/RT of reaction = -88.649

Af/Ar = 2.060E-05

T (K)	delta H (kcal)	del S/R	(Af/Ar)	del G/RT
300.000	-5.892E+01	-1.080E+01	2.030E-05	-8.803E+01
500.000	-5.969E+01	-1.180E+01	7.475E-06	-4.827E+01
800.000	-6.039E+01	-1.238E+01	4.200E-06	-2.561E+01
1000.000	-6.050E+01	-1.244E+01	3.947E-06	-1.800E+01
1200.000	-6.025E+01	-1.233E+01	4.417E-06	-1.294E+01
1500.000	-5.920E+01	-1.194E+01	6.506E-06	-7.920E+00
2000.000	-5.682E+01	-1.125E+01	1.302E-05	-3.049E+00

Table XV : Thermodynamic analysis for reaction in Figure 8

APPENDIX D

QRRK INPUT PARAMETERS

TABLE XVI: Input parameters for QRRK Calculation
 (Phenoxy + tetrachlorobenzene----->
 Cl + trichlorobiphenyl ether)

k	A ^f	E kcal/mol	reference
1	7.0E12	4.0	a
-1	1.35E15	9.47	b
2	3.33E13	5.17	c
<ν> = 604.46 cm ⁻¹			d
LJ parameters: σ = 7.06 Å, ε/k = 599.5			e

a: A factor 1/8 (O + CC*CC) from Kerr et al, E factor average O addition to olefin from Kerr et. al.(37).

b: A₁ calculated from thermodynamics and microreversibility.

c: A₂ calculated from thermodynamics and 1/2 reverse A factor of Cl + C*C from Kerr et. al.(37), E₂ is enthalpy change plus E_a for typical Cl addition to olefin (1.4 kcal/mol) from Kerr et al(37).

d: <ν> is obtained from the output of CPFIT(5).

e: σ and ε/k are estimated

f: Units are cm³ s⁻¹ mol⁻¹ for bimolecular reactions and s⁻¹ for unimolecular reactions

TABLE XVII: Input parameters for QRRK Calculation
 (Oxygen atom + hexachlorobiphenyl ----->
 H + hexachlorophenylphenoxy radical)

k	A ^f	E kcal/mol	reference
1	1.1E13	3.5	a
-1	2.58E13	26.58	b
2	1.71E12	4.00	c
<ν> = 578.06 cm ⁻¹			d
LJ parameters: σ = 7.01 Å, ε/k = 851.8			e

a: A factor 0.55 (O + Cl benzene addition), value from Herron et. al.(38), E₁ typical O addition to olefin from Kerr et. al.(37).

b: A₁ calculated from thermodynamics and microreversibility.

c: A₂ calculated from thermodynamics and reverse A factor of H addition to chloro olefin, E factor of typical H addition to olefin (4 kcal/mol) from Kerr et. al.(37)

d: <ν> is obtained from the output of CPFIT(5).

e: σ and ε/k are estimated

f: Units are cm³ s⁻¹ mol⁻¹ for bimolecular reactions and s⁻¹ for unimolecular reactions

TABLE XVIII: Input parameters for QRRK Calculation
 (heptachlorophenyl phenoxy radical ----->
 Cl + hexachlorodibenzo furan)

k	A ^f	E kcal/mol	reference
1	2.14E12	8.73	a
-1	1.95E11	11.24	b
2	9.04E11	9.70	c

< ν > = 737.82 cm⁻¹ d

LJ parameters: σ = 7.01 A, ϵ/k = 851.8 e

- a: A factor calculated from transition state theory with ΔS of -4 eu, E₁ is ring strain (5.23 kcal/mol) + 3.5 kcal/mol
- b: A₋₁ calculated from thermodynamics and microreversibility.
- c: A₂ calculated from thermodynamics and 1/2 reverse A factor of Cl addition to C*C, E factor of typical Cl addition to olefin (1.4 kcal/mol) from Kerr et. al.(37)
- d: < ν > is obtained from the output of CPFIT(5)
- e: σ and ϵ/k are estimated
- f: Units are cm³ s⁻¹ mol⁻¹ for bimolecular reactions and s⁻¹ for unimolecular reactions

TABLE XIX: Input parameters for QRRK Calculation
 (Oxygen atom + trichlorobiphenyl ether ----->
 H + trichlorophenylphenoxy ether radical)

k	A ^f	E kcal/mol	reference
1	1.1E13	3.5	a
-1	1.2E14	20.68	b
2	1.71E12	4.00	c

< ν > = 482.66 cm⁻¹ d

LJ parameters: σ = 7.06 A, ϵ/k = 514.2 e

- a: A factor 0.55 (O + Cl benzene addition), value from Herron et. al.(38), E factor typical O addition to olefin from Kerr et. al.(37).
- b: A₋₁ calculated from thermodynamics and microreversibility.
- c: A₂ calculated from thermodynamics and reverse A factor of H addition to chloro olefin, E₂ typical H addition to olefin (4 kcal/mol) from Kerr et. al.(37).
- d: < ν > is obtained from the output of CPFIT(5).
- e: σ and ϵ/k are estimated
- f: Units are cm³ s⁻¹ mol⁻¹ for bimolecular reactions and s⁻¹ for unimolecular reactions

TABLE XX Input parameters for QRRK Calculation
 (heptachlorophenyl phenoxy ether radical ----->
 Cl + hexachlorodioxin)

k	A ^f	E _{kcal/mol}	reference
1	1.0E12	6.8	a
-1	1.59E15	26.6	b
2	3.84E14	22.05	c

< ν > = 723 cm⁻¹ d

LJ parameters: $\sigma = 7.37 \text{ \AA}$, $\epsilon/k = 855.7$ e

a: A₁ calculated from transition state theory with ΔS of -5.5 eu due to loss of rotor, E₁ is ring strain + 3.5

b: A₋₁ is calculated from thermodynamics and microreversibility.

c: A₂ is calculated from thermodynamics and 1/2 reverse A factor of Cl addition to C*Cl (1.58E13), E₂ typical Cl addition to olefin from Kerr et. al.(37)

d: < ν > is obtained from the output of CPFIT(5).

e: σ and ϵ/k are estimated

f: Units are cm³ s⁻¹ mol⁻¹ for bimolecular reactions and s⁻¹ for unimolecular reactions

APPENDIX E

ENERGY LEVEL DIAGRAMS AND THERMODYNAMIC DATA

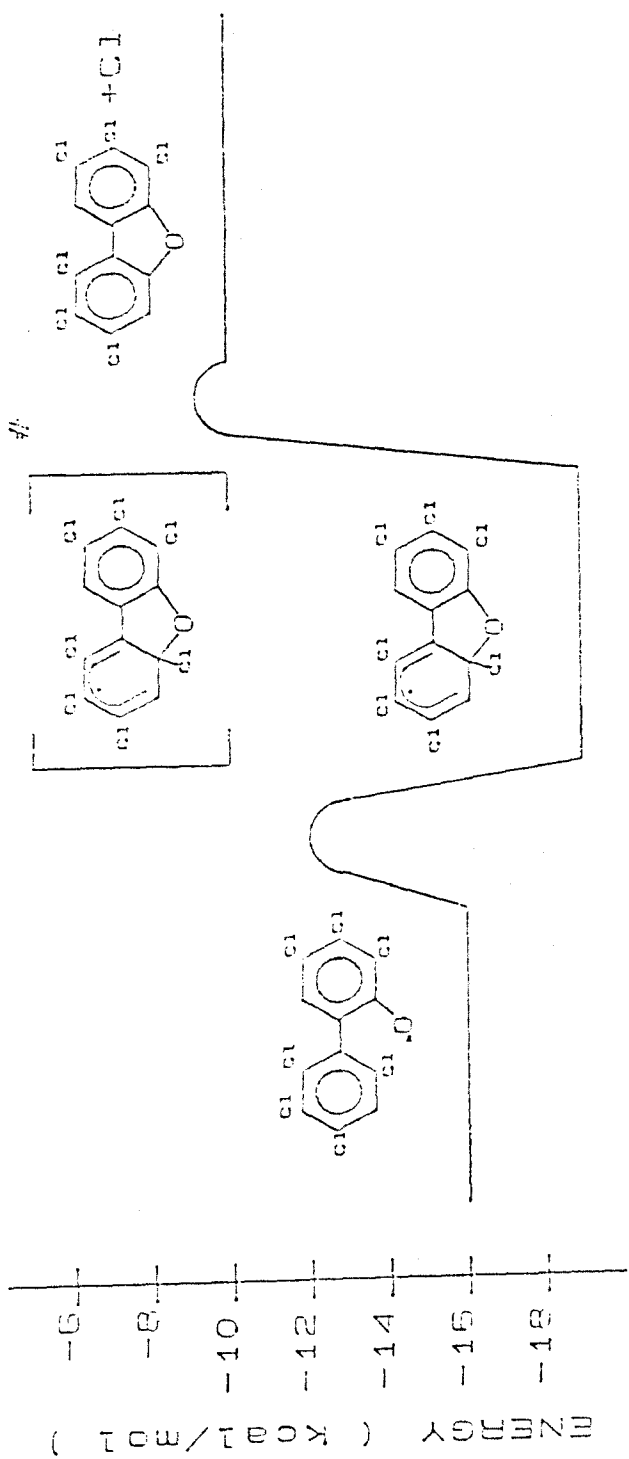


Figure 1: Energy level diagram for isomerization of heptachlorinated phenoxyphenyl radical

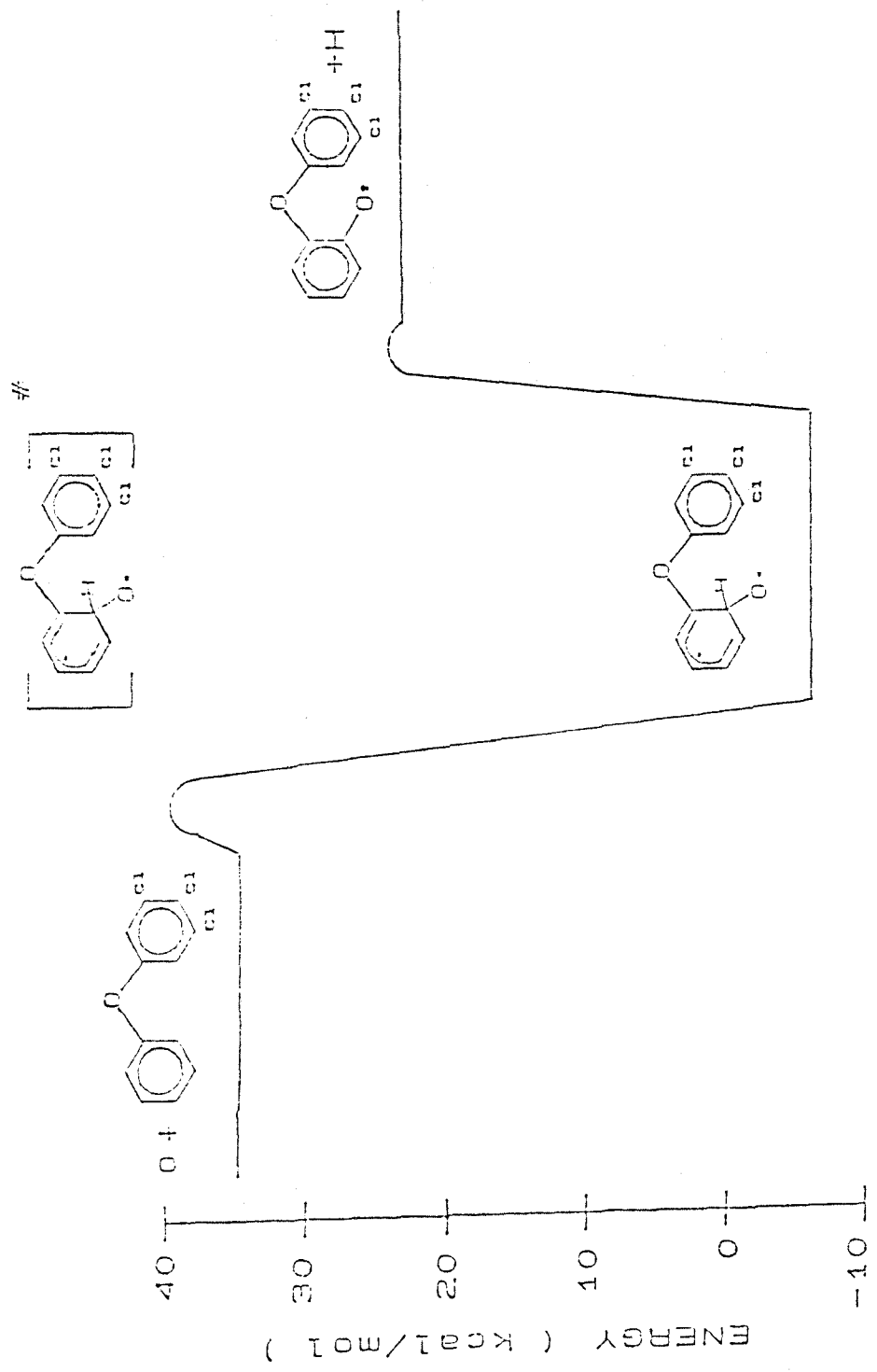


Figure 2: Energy level diagram for oxygen addition to trichlorinated diphenoxy ether

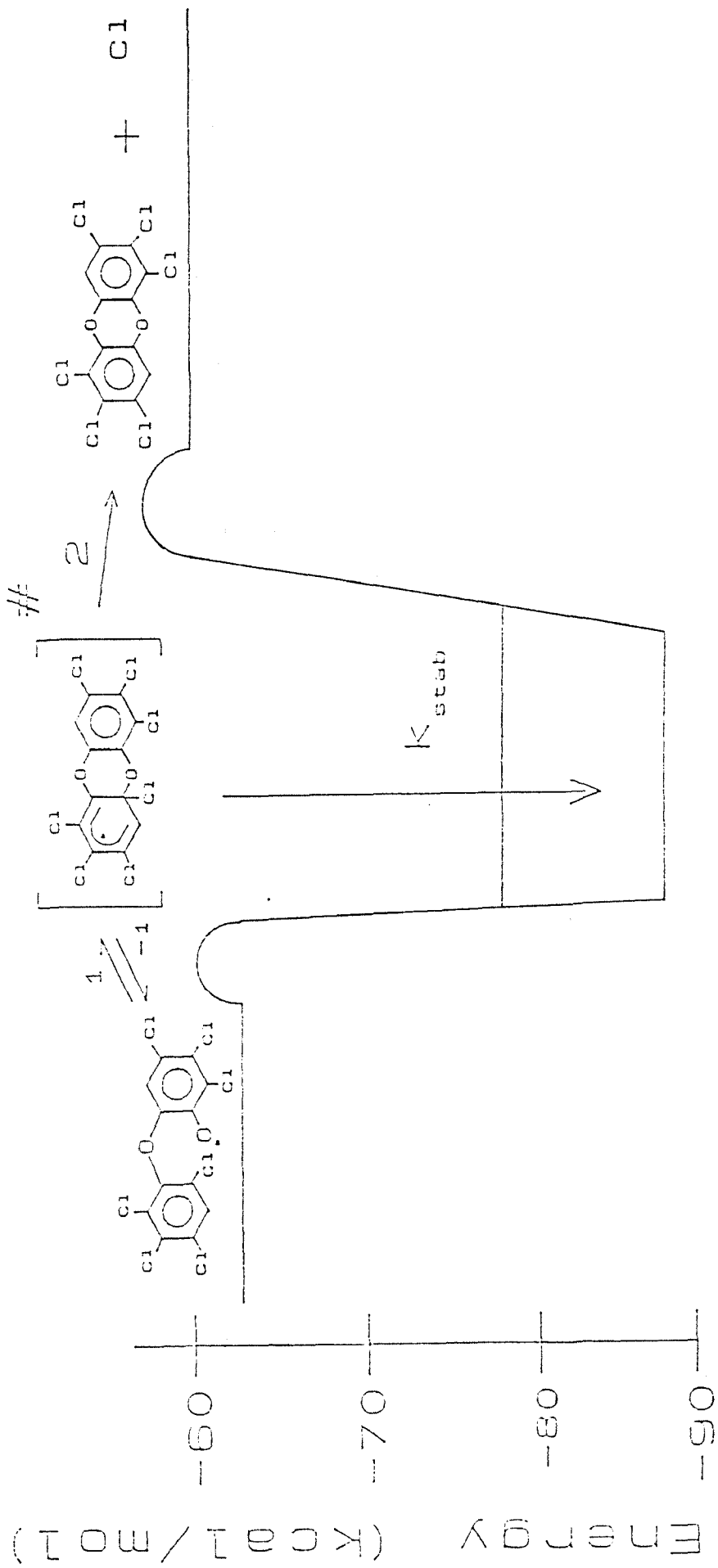


Figure 3: Energy level diagram for isomerization of heptachlorinated phenoxyphenylether radical

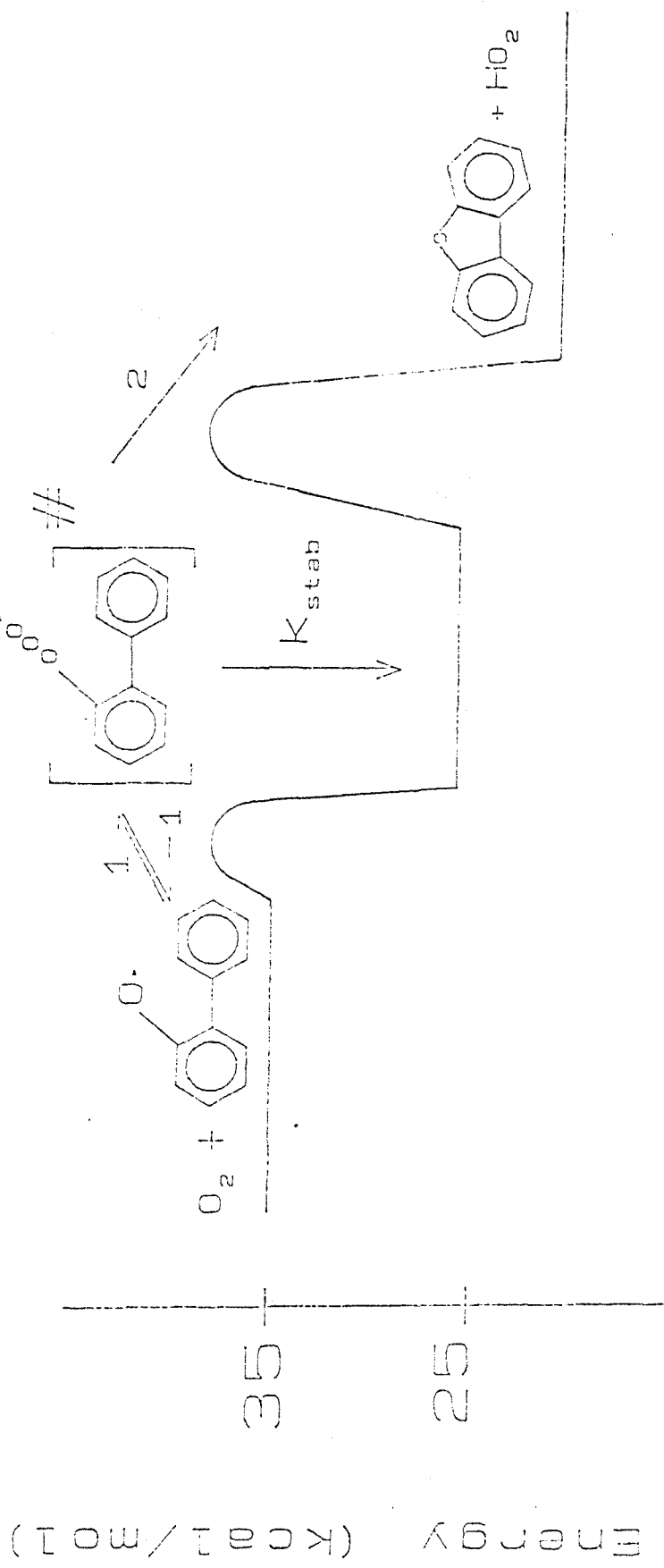


Figure 4: Energy level diagram for molecular oxygen addition to phenoxyl radical

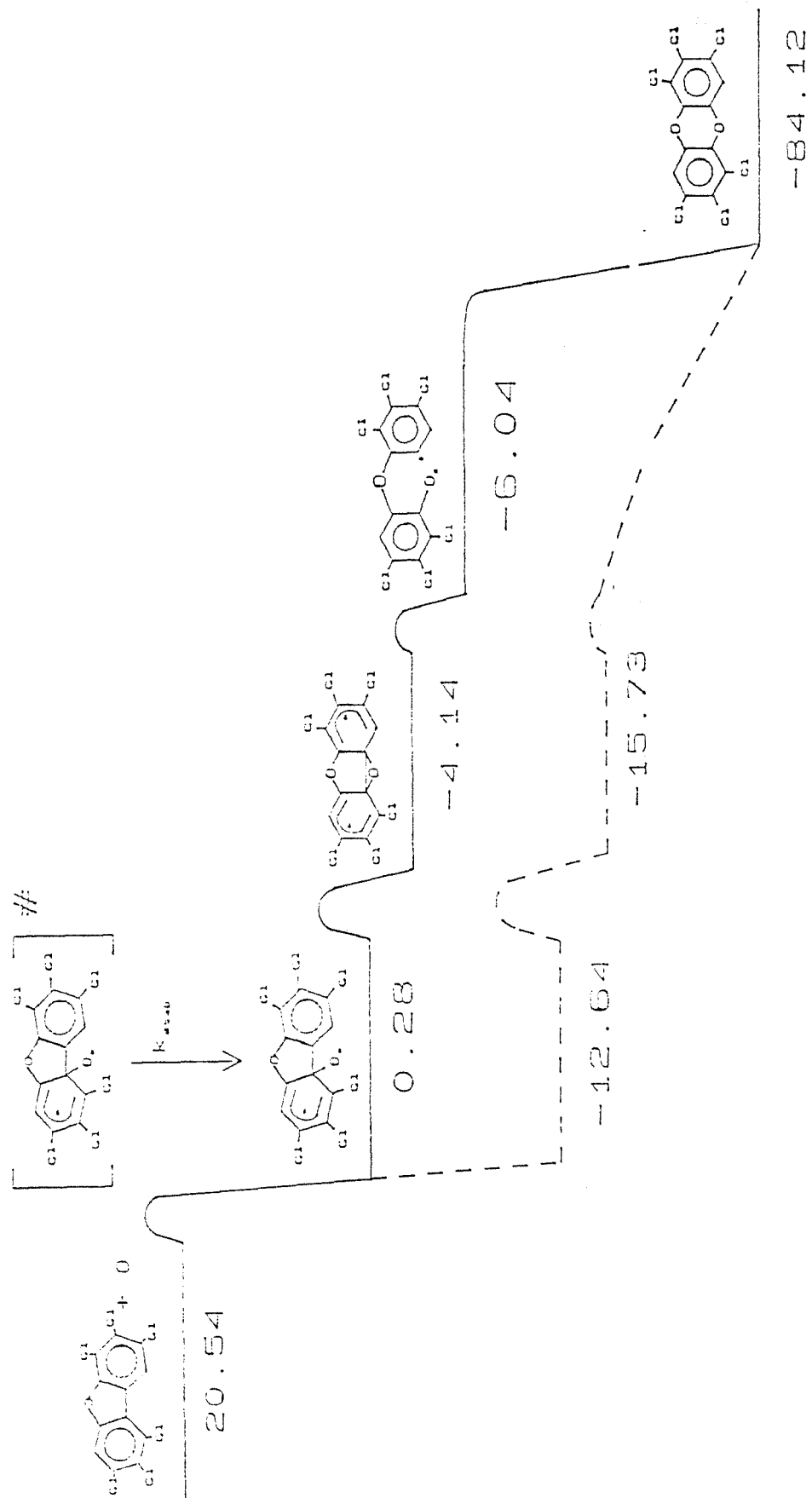


Figure 5: Energy level diagram for oxygen addition to hexachlorinated dibenzofuran

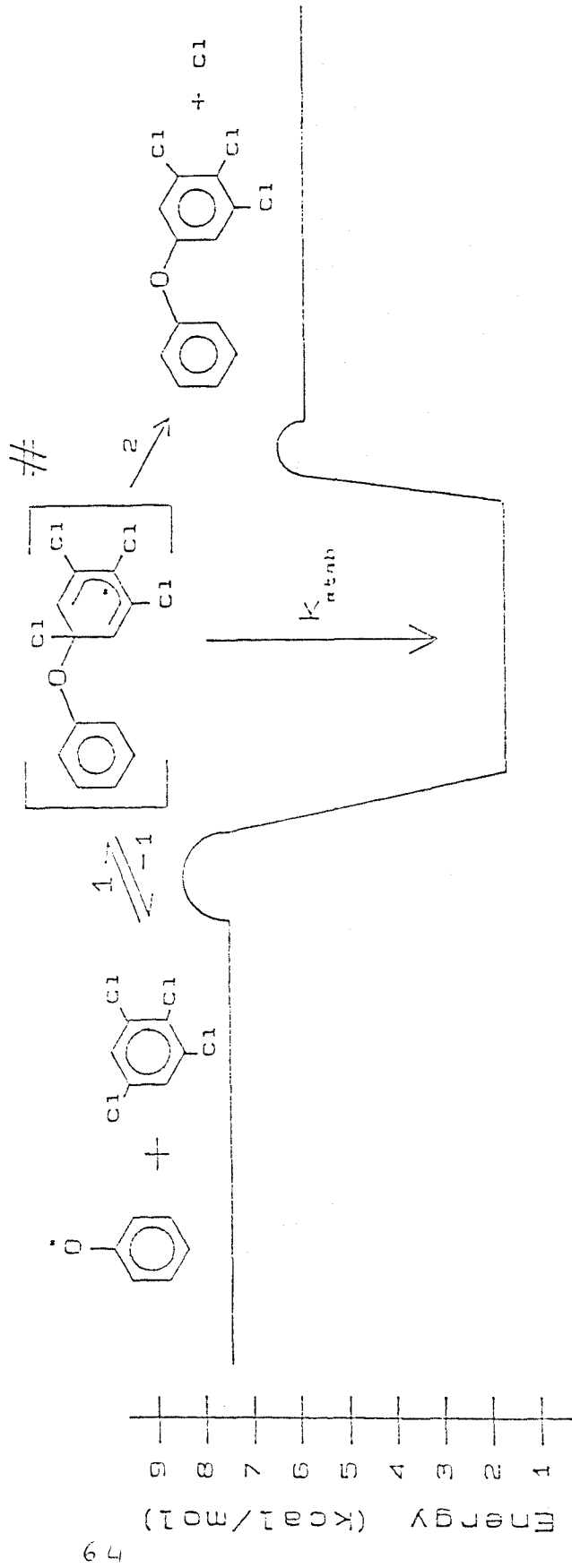


Figure 6: Energy level diagram for reaction of phenoxy with tetrachlorobenzene

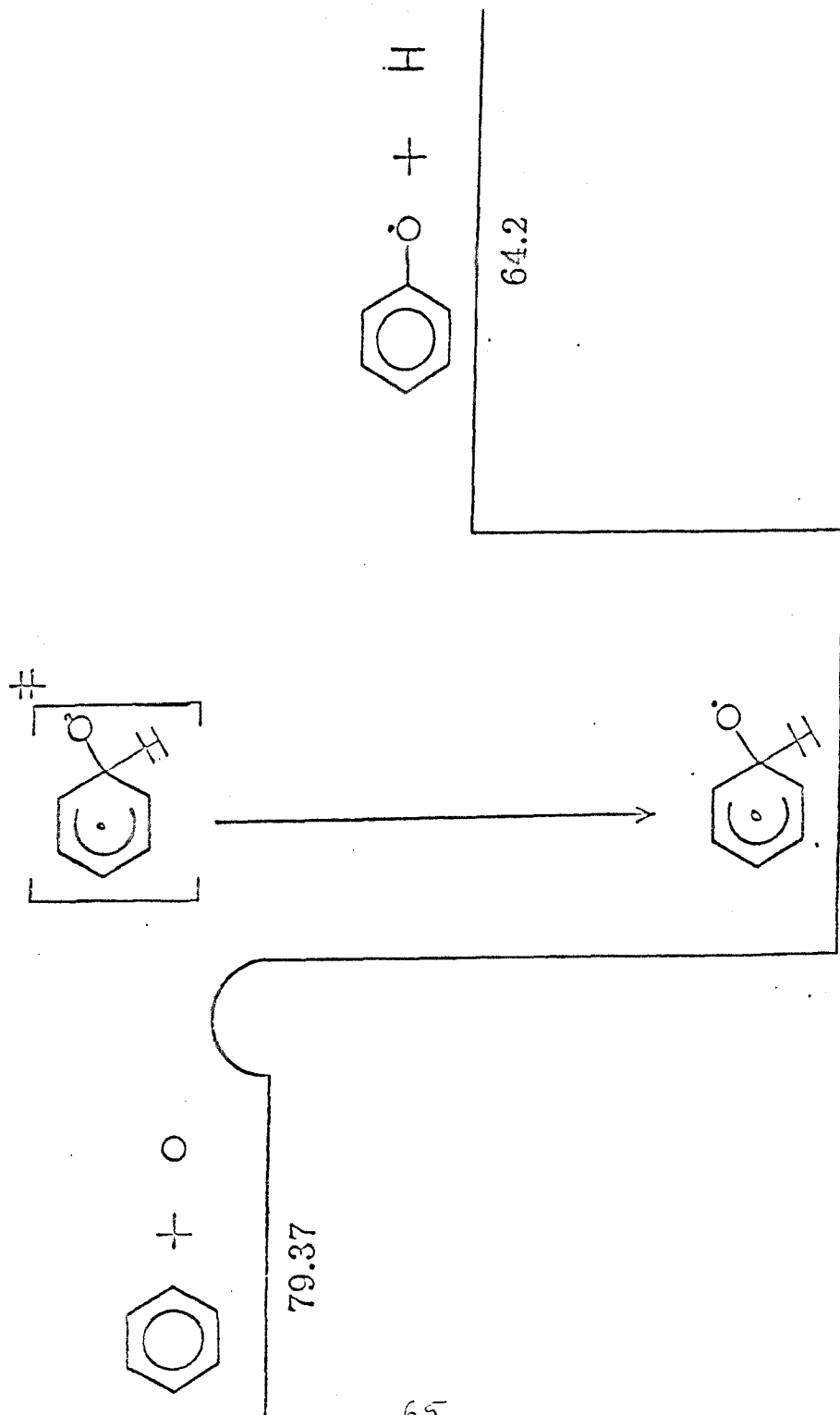


Figure 7: Energy level diagram for oxygen addition to benzene

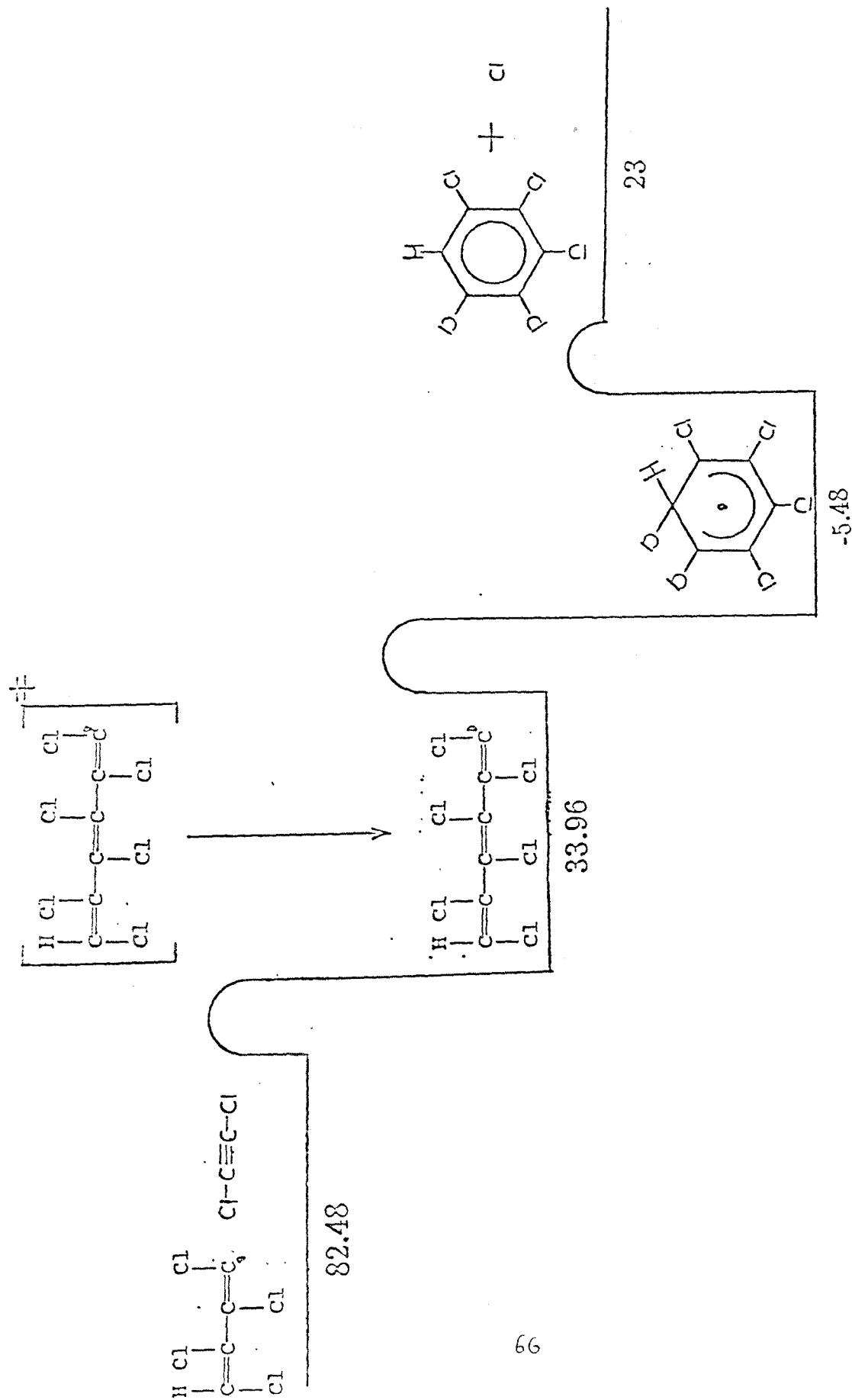
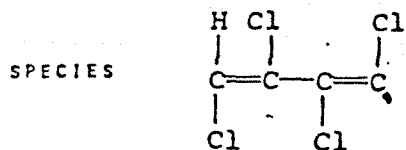
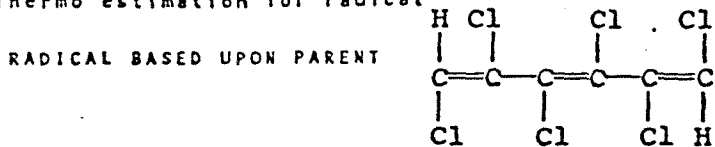


Figure 8: Energy level diagram for formation of pentachlorobenzene



Thermo estimation for radical



C4HCL4

PARENT FORMULA

PARENT SYMMETRY 1

UNITS:KCAL

GROUPS 3

Gr # - GROUP ID - Quantity

1 - CD/CL/CD - 2

2 - CD/CL/H - 2

3 - VIN - 1

Hf	S	Cp	300	500	800	1000	1500	2000
41.08	97.46	31.74	39.61	43.85	45.05	45.88	47.28	

CPINF = 49.67

SYMMETRY 1

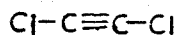
R ln(2) has been added to S to account for unpaired electron

BOND 102.70

DELTA BOND ENERGY = -2.840

ENDSPECIES

SPECIES



Thermo estimation for molecule

C2CL2

UNITS:KCAL

GROUPS 1

Gr # - GROUP ID - Quantity

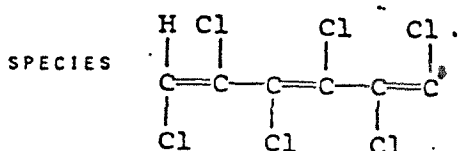
1 - CT/CL - 2

Hf	S	Cp	300	500	800	1000	1500	2000
41.40	65.42	15.80	17.40	18.80	19.20	19.70	19.76	

CPINF = 19.87

SYMMETRY 2

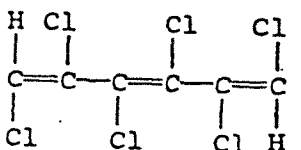
ENDSPECIES



Thermo estimation for radical

RADICAL BASED UPON PARENT

C6HCL6

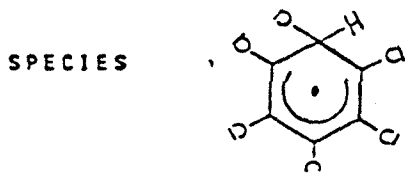


PARENT FORMULA C6H2CL6
 PARENT SYMMETRY 1
 UNITS:KCAL
 GROUPS 3

Gr #	GROUP ID	Quantity
1	CD/CL/CD	- 4
2	CD/CL/H	- 2
3	VIN	- 1

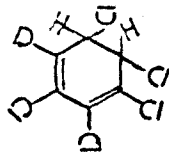
Hf S Cp 300 500 800 1000 1500 2000
 33.96 123.06 47.84 59.79 65.65 67.21 68.96 70.65
 CPINF = 73.52

SYMMETRY 1
 R ln(2) has been added to S to account
 for unpaired electron
 BOND 102.70
 DELTA BOND ENERGY = -2.840
 ENDSPECIES



Thermo estimation for Radical

RADICAL BASED UPON PARENT



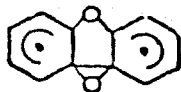
PARENT FORMULA C6H2CL6
 PARENT SYMMETRY 1
 UNITS:KCAL
 GROUPS 6

Gr #	GROUP ID	Quantity	Gr #	GROUP ID	Quantity
1	CD/CL/C	- 2	4	CY/C6/DE/13	- 1
2	CD/CL/CD	- 2	5	ORT/CL/CL	- 4
3	C/CL/CD/C/H	- 2	6	CHD	- 1

Hf S Cp 300 500 800 1000 1500 2000
 -5.48 116.07 39.97 53.01 62.77 65.30 74.98 74.44
 CPINF = 73.52

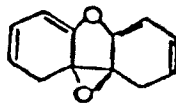
SYMMETRY 1
 R ln(2) has been added to S to account
 for unpaired electron
 BOND 72.60
 DELTA BOND ENERGY = -3.960
 ENDSPECIES

SPECIES



Thermo estimation for diradical

RADICAL BASED UPON PARENT



C12H8O2

PARENT FORMULA

C12H10O2

PARENT SYMMETRY

UNITS:KCAL

GROUPS 12

Gr #	GROUP ID	Quantity	Gr #	GROUP ID	Quantity
1	CD/CD/H	- 4	7	O/C2	- 1
2	CD/C/H	- 2	8	CY/C6/DE/13	- 2
3	CD/C/O	- 2	9	CY/C4O	- 1
4	O/CD2	- 1	10	CY/C2O	- 1
5	C/CD/C2/O	- 2	11	CHD	- 1
6	C/CD/C/H2	- 2	12	CHD	- 1

Hf S Cp 300 500 800 1000 1500 2000
 71.47 98.16 38.17 66.76 91.33 100.05 114.04 118.90
 CPINF = 127.17

SYMMETRY 1

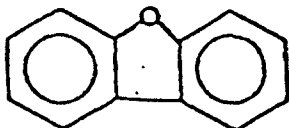
R ln(2) has been added to S to account for unpaired electron

BOND 76.56

SYMMETRY

ENDSPECIES

SPECIES



Thermo estimation for molecule

C12H8O

UNITS:KCAL

GROUPS 5

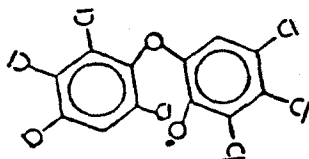
Gr #	GROUP ID	Quantity
1	CB/H	- 8
2	CB/CB	- 2
3	CB/O	- 2
4	O/CB2	- 1
5	CY/DBF	- 1

Hf S Cp 300 500 800 1000 1500 2000
 19.90 92.47 36.72 63.18 85.64 94.76 105.19 111.12
 CPINF = 121.21

SYMMETRY 2

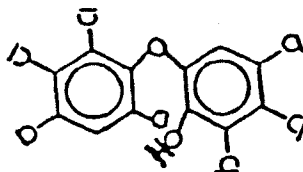
ENDSPECIES

SPECIES



Thermo estimation for radical

RADICAL BASED UPON PARENT



C12H202CL7

PARENT FORMULA

C12H302CL7

PARENT SYMMETRY

1

UNITS:KCAL

GROUPS 11

Gr #	GROUP ID	Quantity	Gr #	GROUP ID	Quantity
1	CB/H	- 2	7	MET/CL/CL	- 1
2	CB/CL	- 7	8	ORT/CL/OH	- 3
3	CB/O	- 3	9	MET/CL/OH	- 4
4	O/CB2	- 1	10	PAR/CL/OH	- 3
5	O/H/C	- 1	11	PHENOXY	- 1
6	ORT/CL/CL	- 4			

Hf S Cp 300 500 800 1000 1500 2000
 -63.13 160.54 72.44 96.13 111.83 117.15 119.09 124.28
 CPINF = 133.13

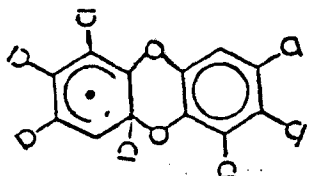
SYMMETRY 1

R ln(2) has been added to S to account for unpaired electron

BOND 86.50

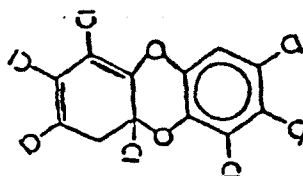
ENDSPECIES

SPECIES



Thermo estimation for radical

RADICAL BASED UPON PARENT



C12H202CL7

PARENT FORMULA

C12H302CL7

PARENT SYMMETRY

1

UNITS:KCAL

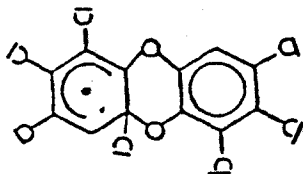
GROUPS 17

Gr #	GROUP ID	Quantity	Gr #	GROUP ID	Quantity
1	CB/H	- 1	10	CD/CL/CD	- 2
2	CB/CL	- 3	11	CY/C6/DE/13	- 1
3	CB/O	- 2	12	CY/C6/E	- 1
4	O/CB/CD	- 1	13	ORT/CL/CL	- 4
5	O/CB/C	- 1	14	ORT/CL/OH	- 2
6	CD/C/O	- 1	15	MET/CL/OH	- 4

7 - C/C/CD/CL/O - 1 | 16 - PAR/CL/OH - 3
 8 - C/CD/C/H2 - 1 | 17 - CHD - 1
 9 - CD/CL/C - 1
 Hf S Cp 300 500 800 1000 1500 2000
 -77.14 145.87 67.91 96.70 115.29 120.24 127.83 129.79
 CPINF = 133.13

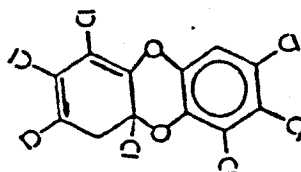
SYMMETRY 1
 R ln(2) has been added to S to account
 for unpaired electron
 BOND 76.56
 ENDSPECIES

SPECIES



Thermo estimation for radical

RADICAL BASED UPON PARENT



C12H202CL7

PARENT FORMULA
 PARENT SYMMETRY 1
 UNITS:KCAL
 GROUPS 17

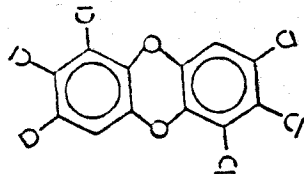
C12H302CL7

Gr #	GROUP ID	Quantity	Gr #	GROUP ID	Quantity
1	CB/H	- 1	10	CD/CL/CD	- 2
2	CB/CL	- 3	11	CY/C6/DE/13	- 1
3	CB/O	- 2	12	CY/C6/E	- 1
4	O/CB/CD	- 1	13	ORT/CL/CL	- 4
5	O/CB/C	- 1	14	ORT/CL/OH	- 2
6	CD/C/O	- 1	15	MET/CL/OH	- 4
7	C/C/CD/CL/O	- 1	16	PAR/CL/OH	- 3
8	C/CD/C/H2	- 1	17	CHD	- 1
9	CD/CL/C	- 1			

Hf S Cp 300 500 800 1000 1500 2000
 -88.72 145.87 67.91 96.70 115.29 120.24 127.83 129.79
 CPINF = 133.13

DELTA EDIT
 -11.58 .00 .00 .00 .00 .00 .00
 SYMMETRY 1
 R ln(2) has been added to S to account
 for unpaired electron
 BOND 76.56
 ENDSPECIES

SPECIES



Thermo estimation for molecule

C12H202CL6

UNITS:KCAL

GROUPS 9

Gr #	GROUP ID	Quantity	Gr #	GROUP ID	Quantity
1	CB/H	- 2	6	ORT/CL/CL	- 4
2	CB/CL	- 6	7	ORT/CL/OH	- 2
3	CB/O	- 4	8	MET/CL/OH	- 5
4	O/CB2	- 2	9	PAR/CL/OH	- 4
5	CY/C6/DE/14	- 1			

Hf S Cp 300 500 800 1000 1500 2000
-91.13 136.14 62.72 89.10 107.23 112.73 117.24 120.91
CPIHF = 127.17

SYMMETRY 2

ENDSPECIES

Figure 9: Thermodynamic data output

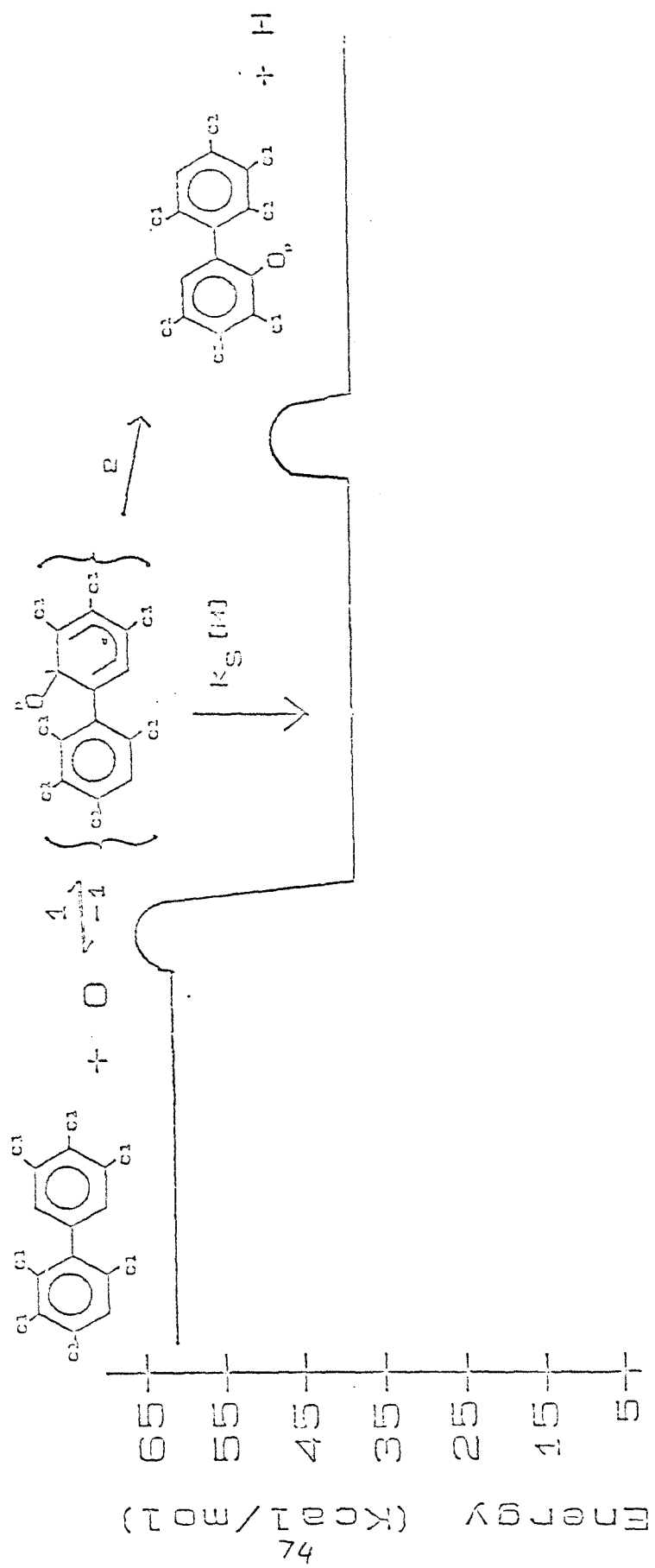


Figure 10: Energy level diagram for oxygen addition to heptachlorinated diphenyl

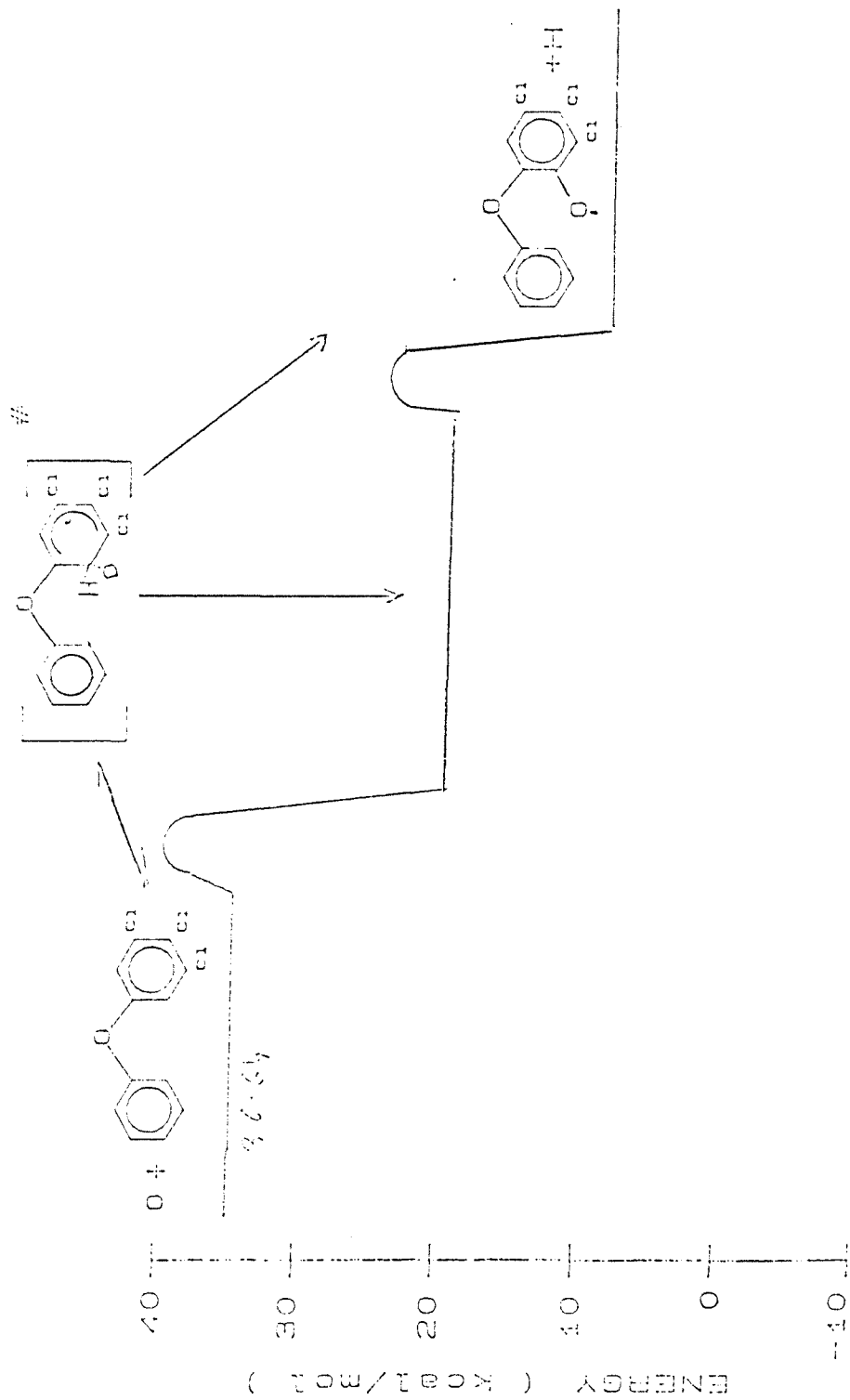


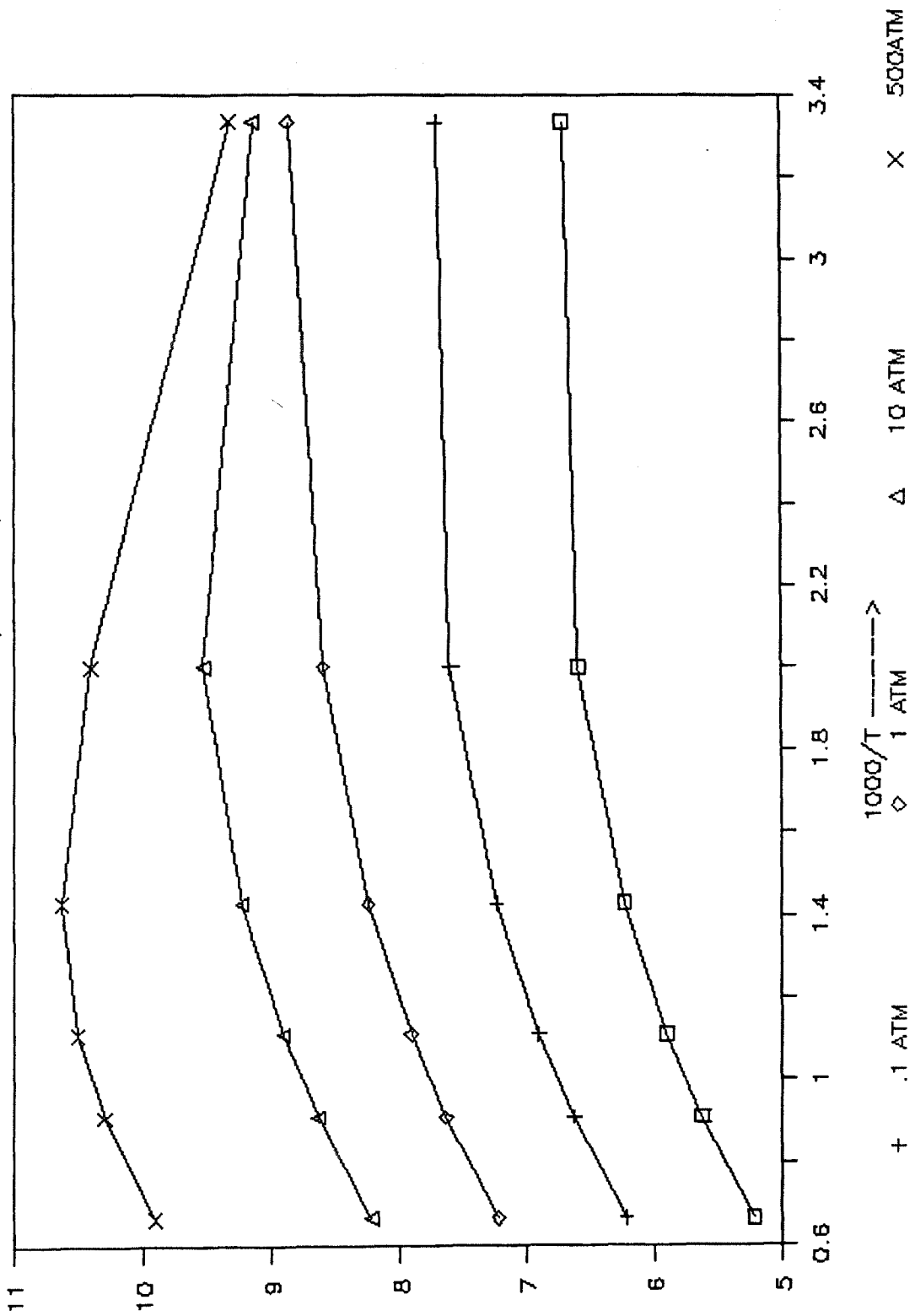
Figure 11: Energy level diagram for oxygen addition to trichlorinated diphenylether on the chlorinated ring

APPENDIX F

QRRK ANALYSIS OUTPUT GRAPHS

G1-A

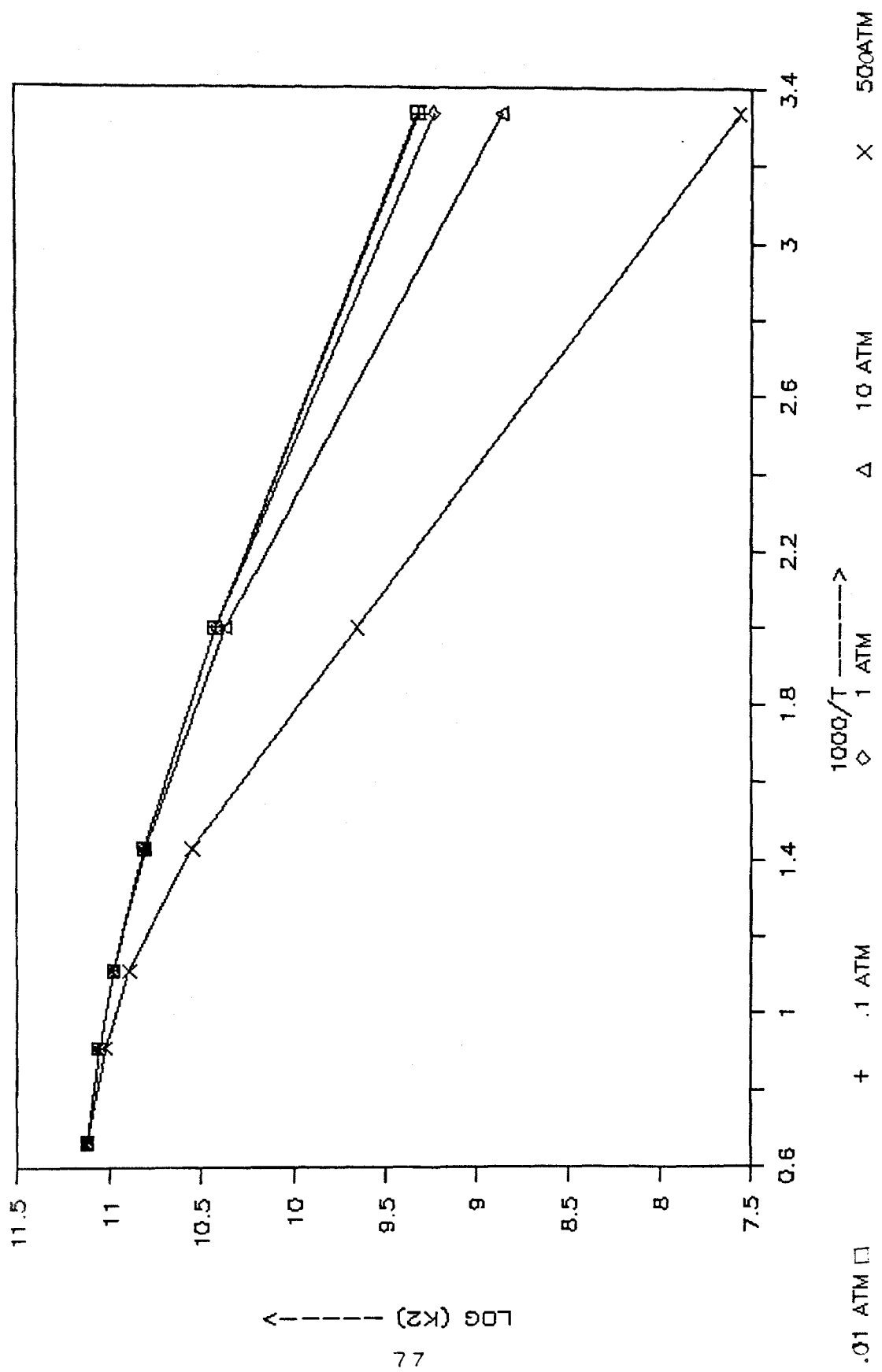
Cl BZ + PHENOXY \rightarrow (COMPLEX)_s



LOG (K1) \leftarrow

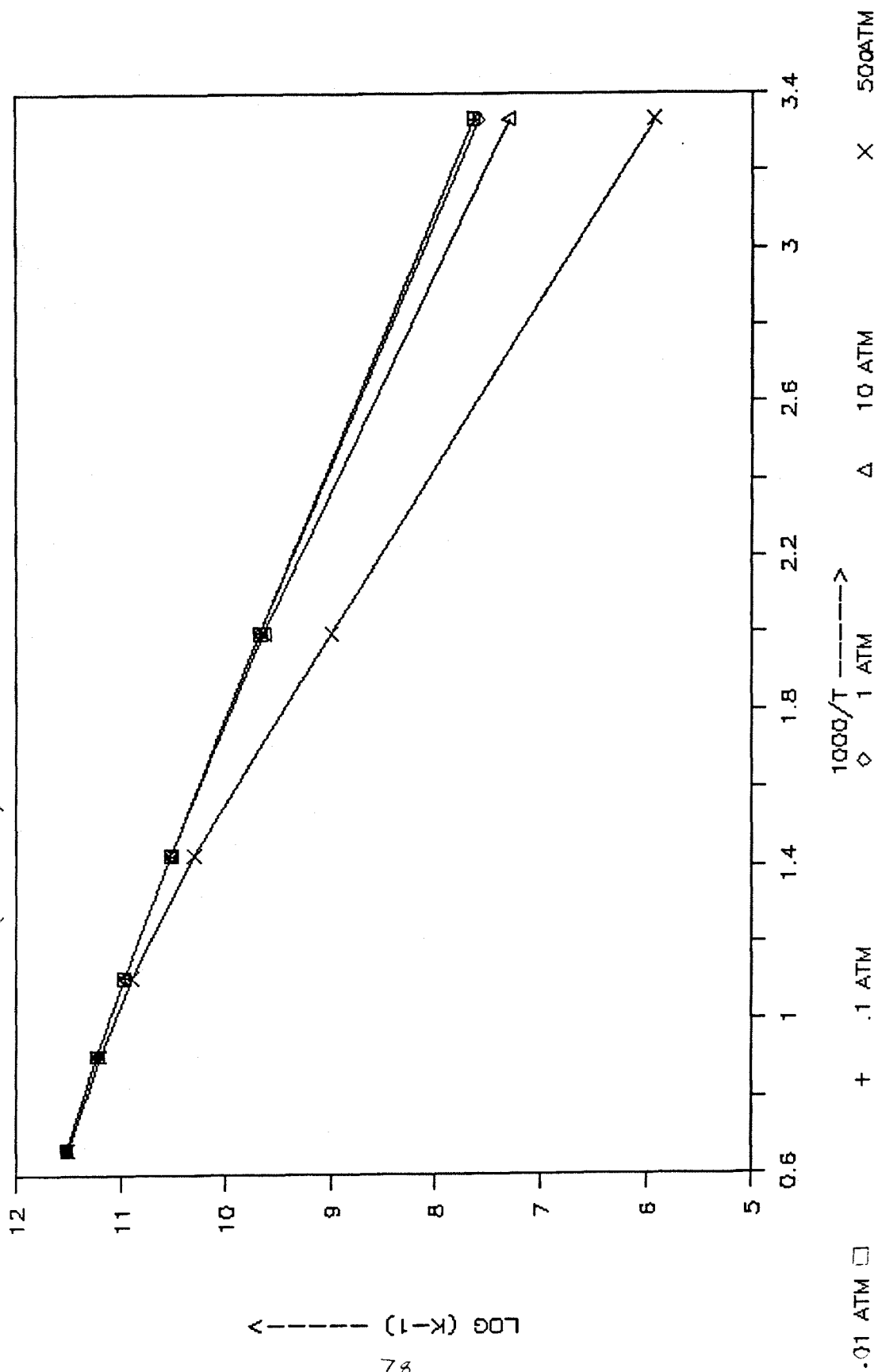
GRAPH G1-B

PHENOXY + CL BZ → Cl + Cl BYPH. ETHER



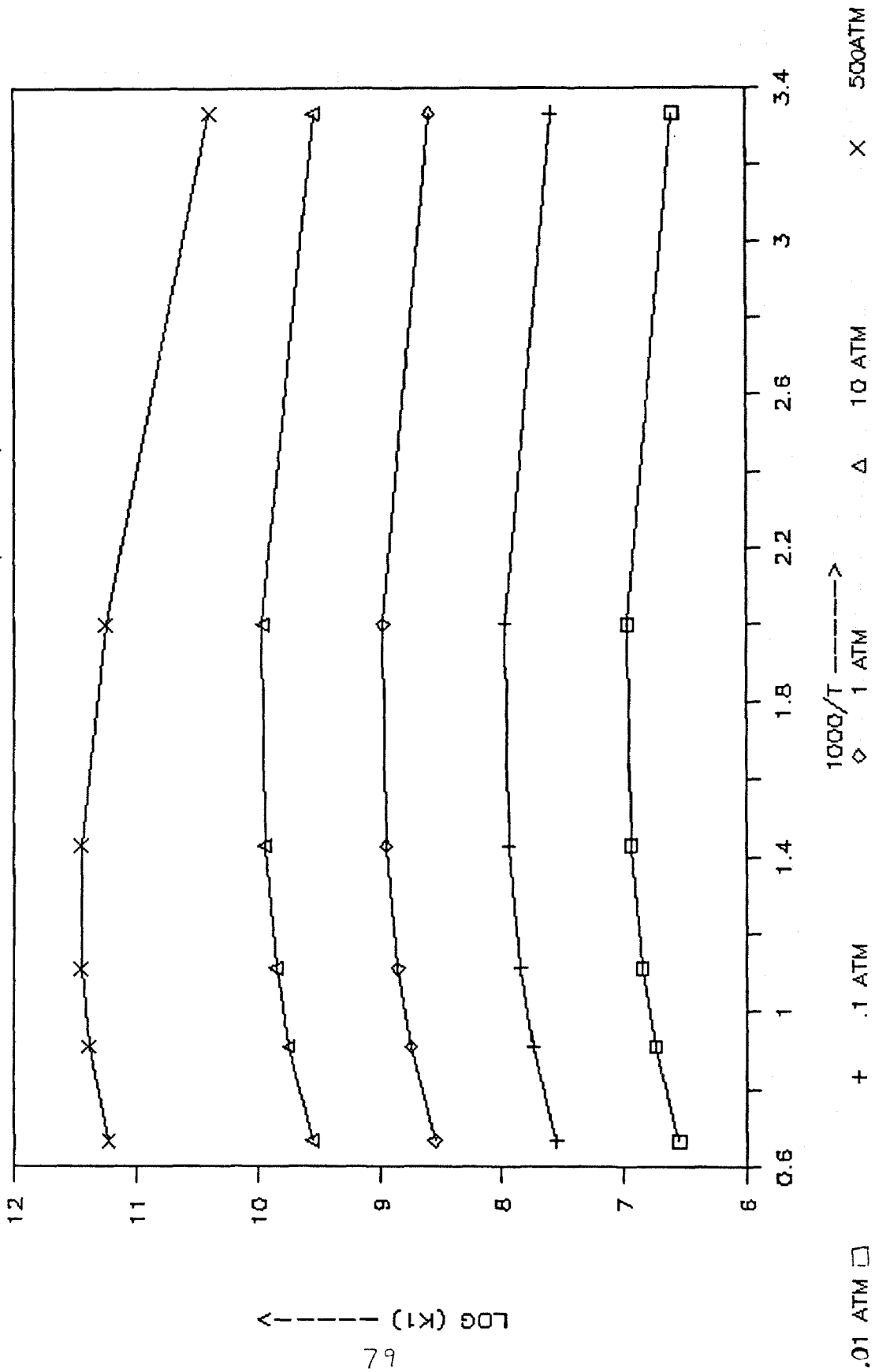
G1-C

(COMPLEX)e $\xrightarrow{\text{Cl BZ} + \text{PHENOXY}}$



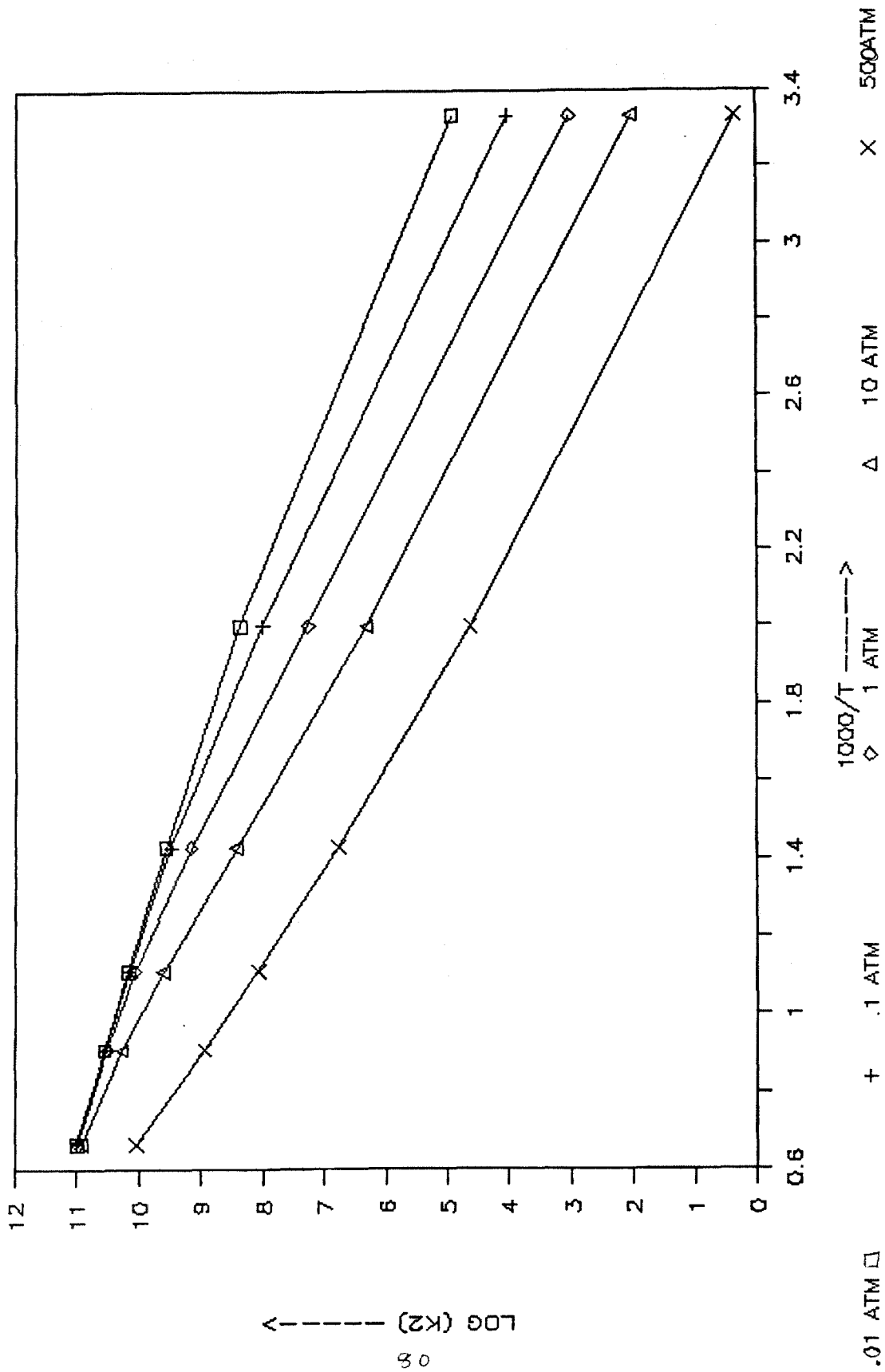
G2-A

O + Cl BYPHENYL \dashrightarrow (COMPLEX)s



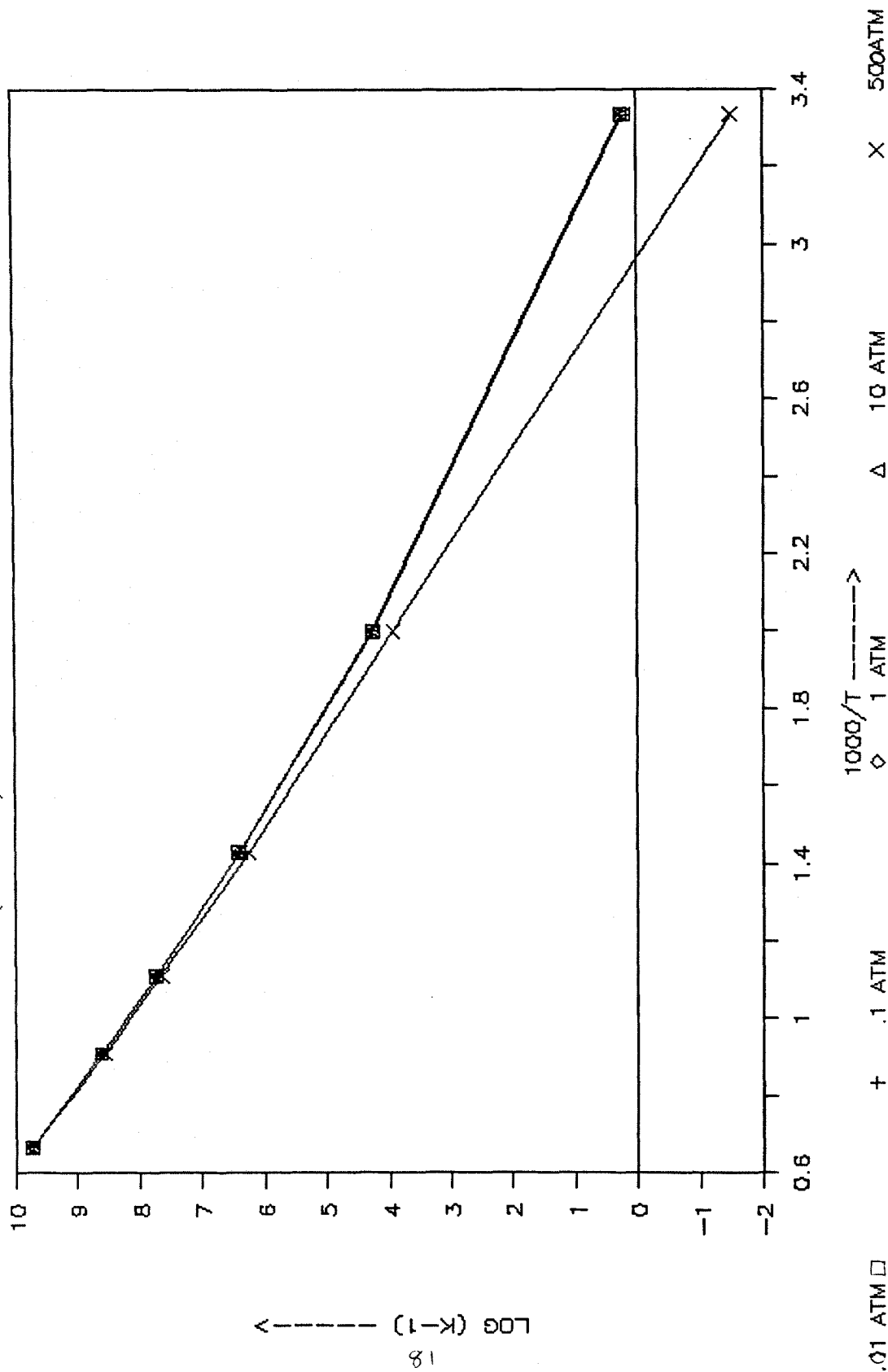
G3-B

CL PH. PHENOXY \rightarrow CI + CI DBF



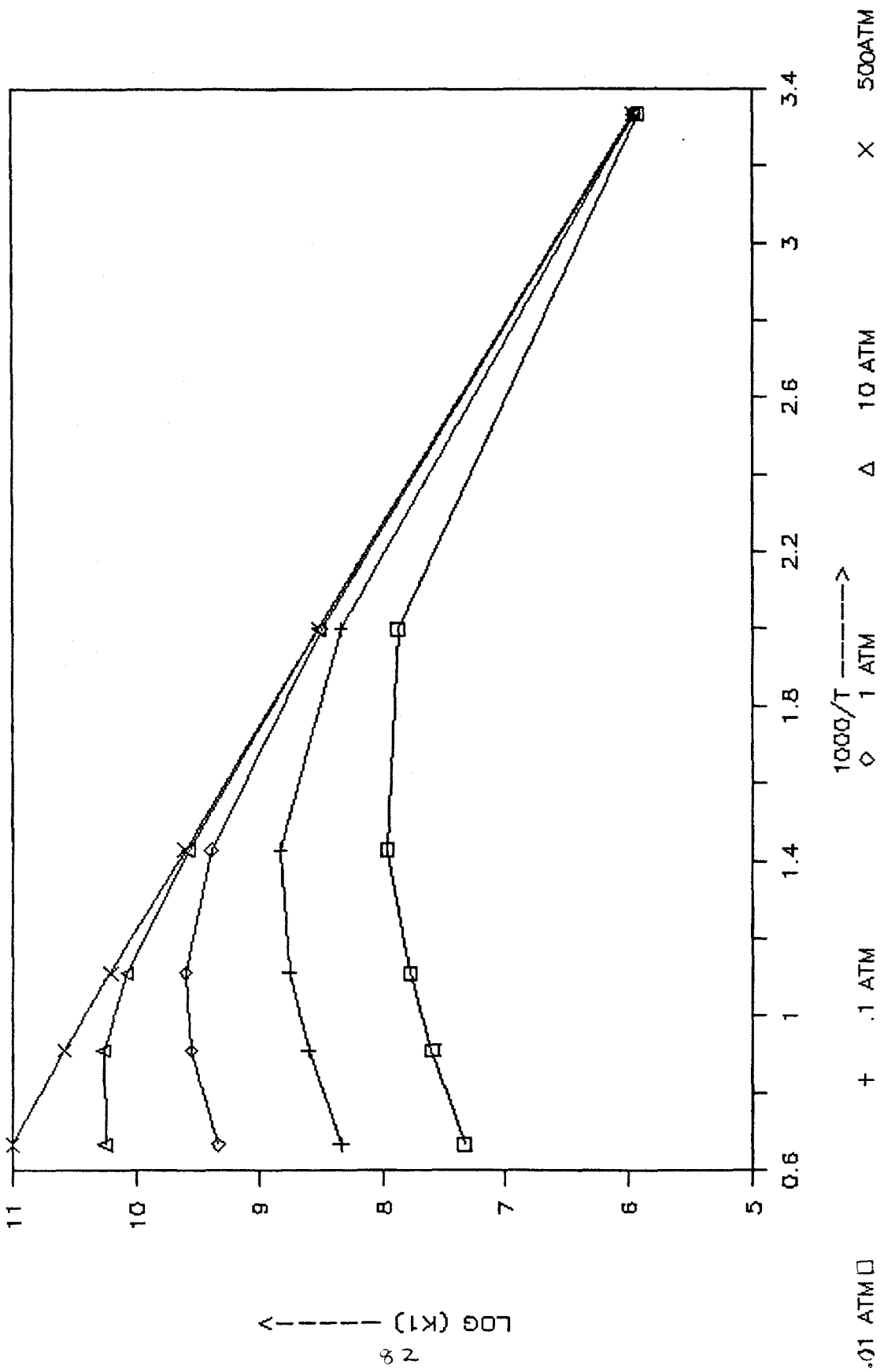
G2-C

(COMPLEX)_e → O + Cl BYPHENYL



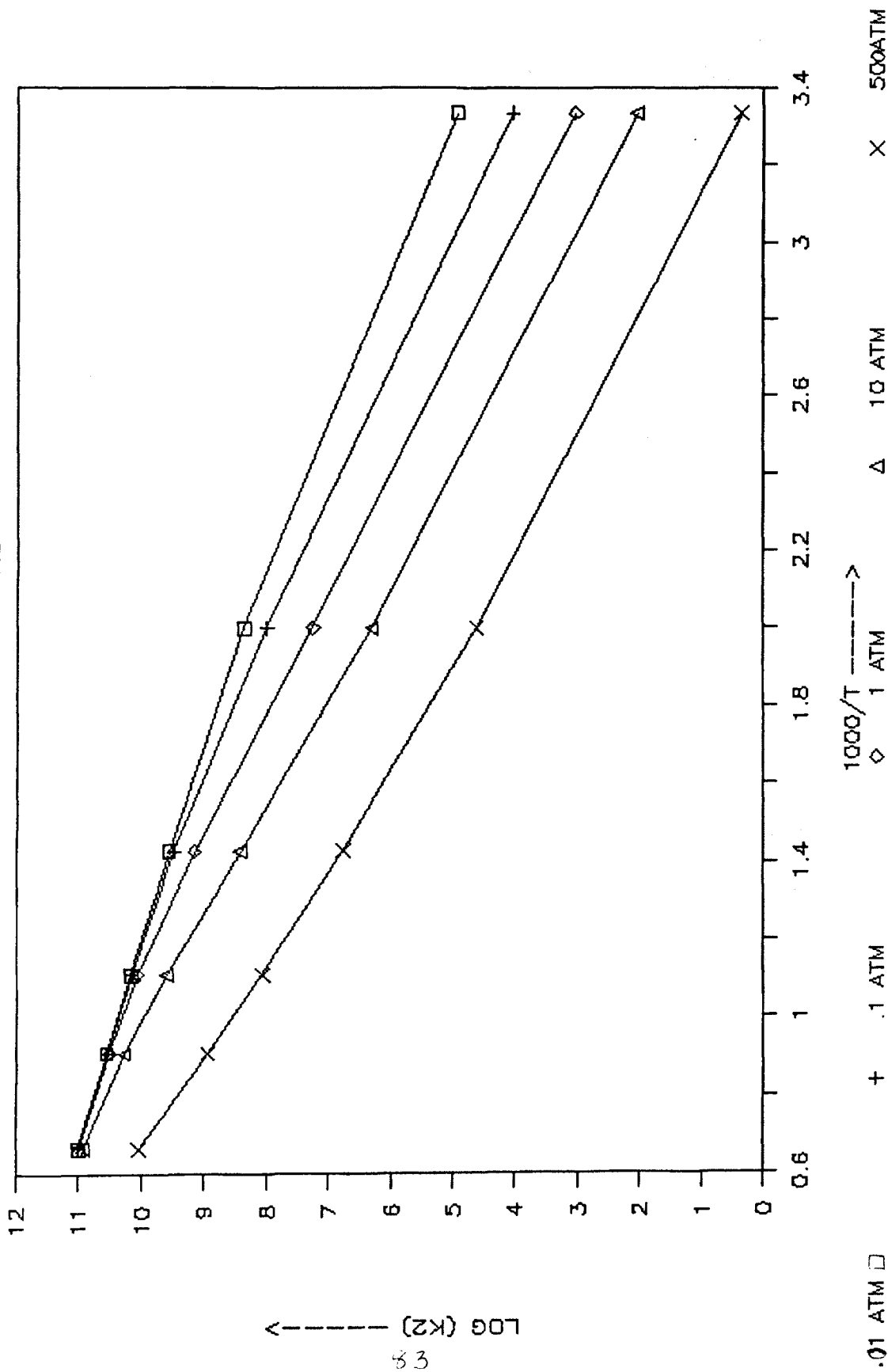
G3-A

GI PH. PHENOXY \longrightarrow (COMPLEX)s



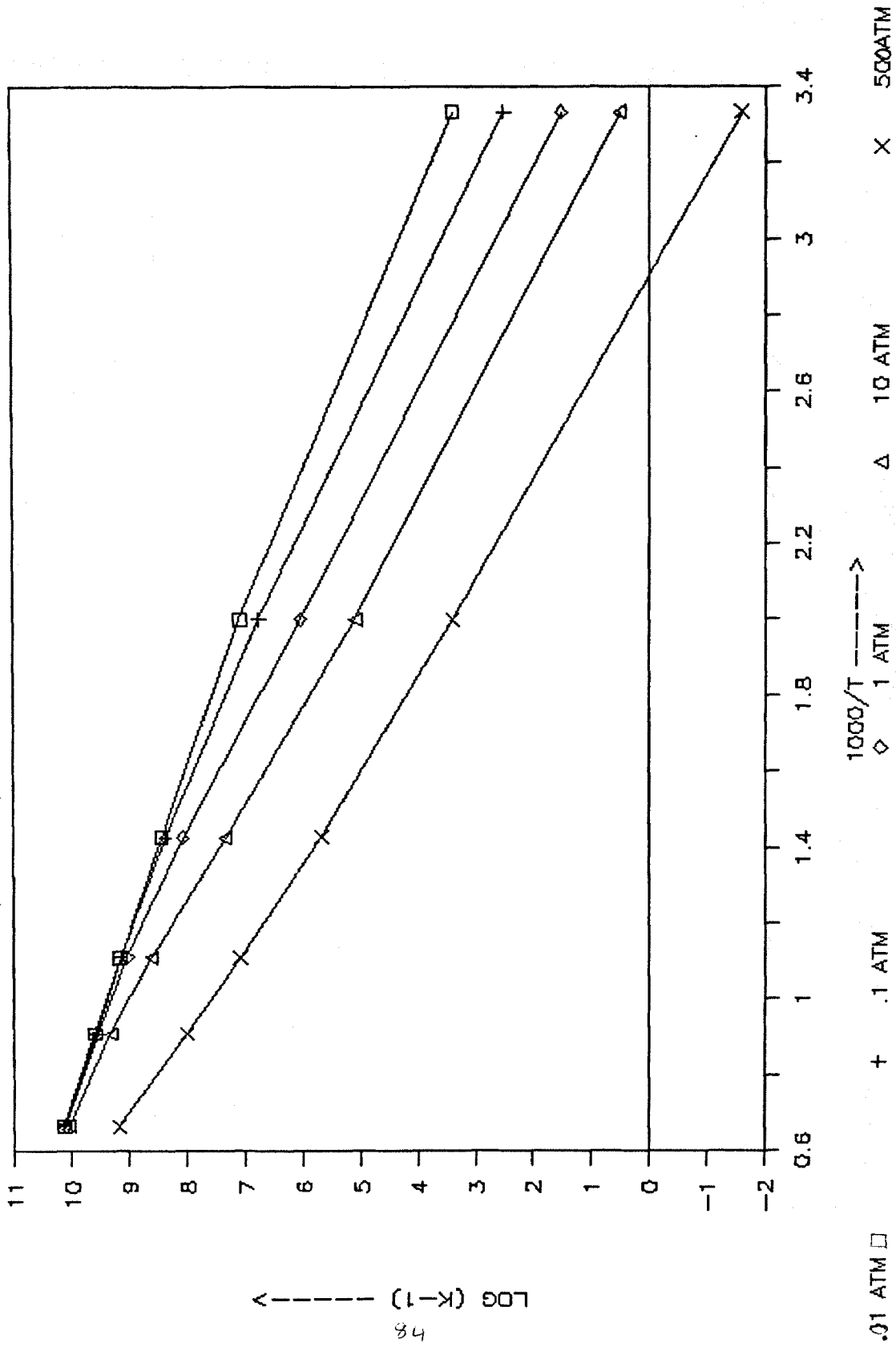
GRAPH G3-B

REACTANTS -----> PRODUCTS



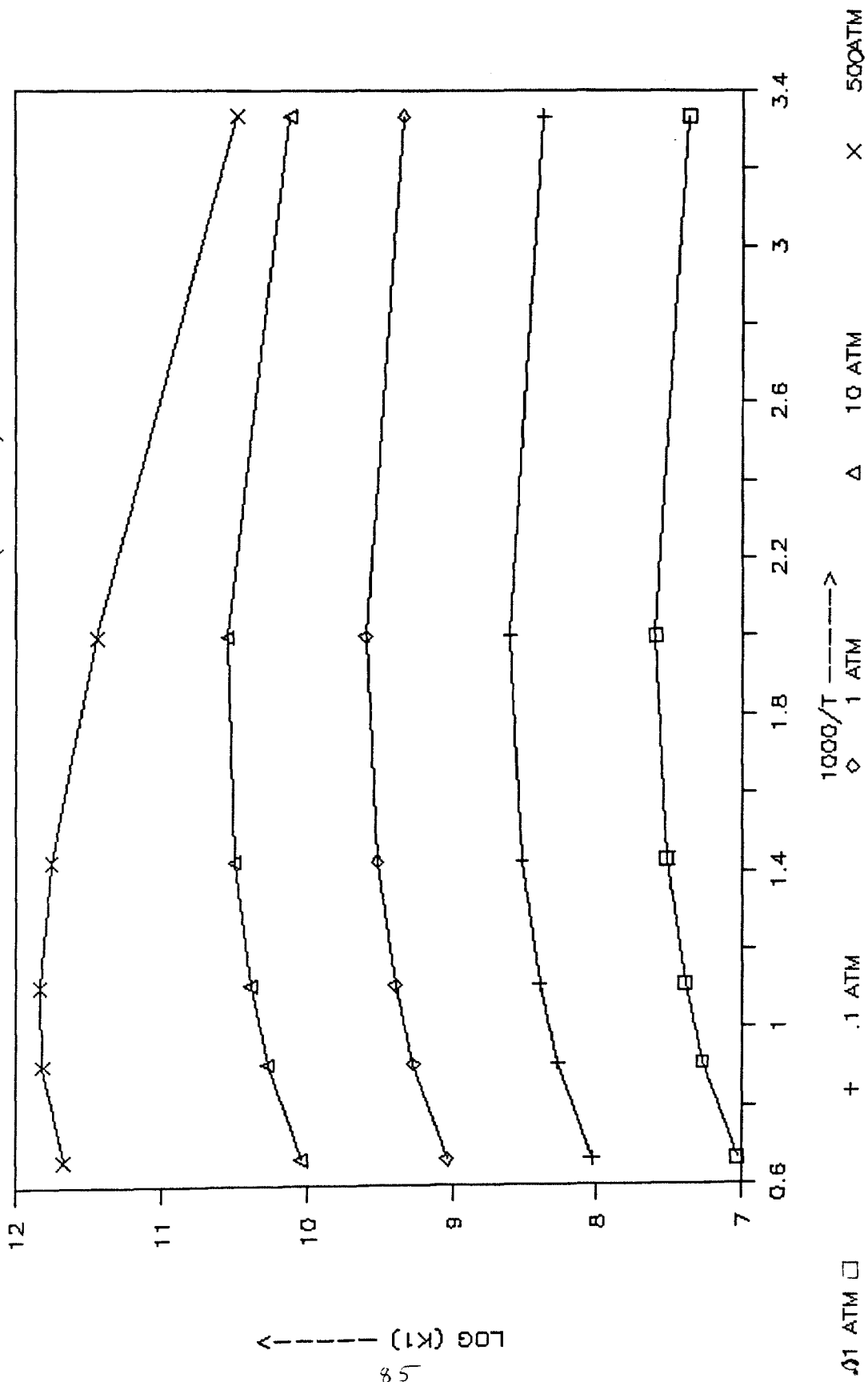
G3-C

(COMPLEX)e -----> CI PHENYL PHENOXY



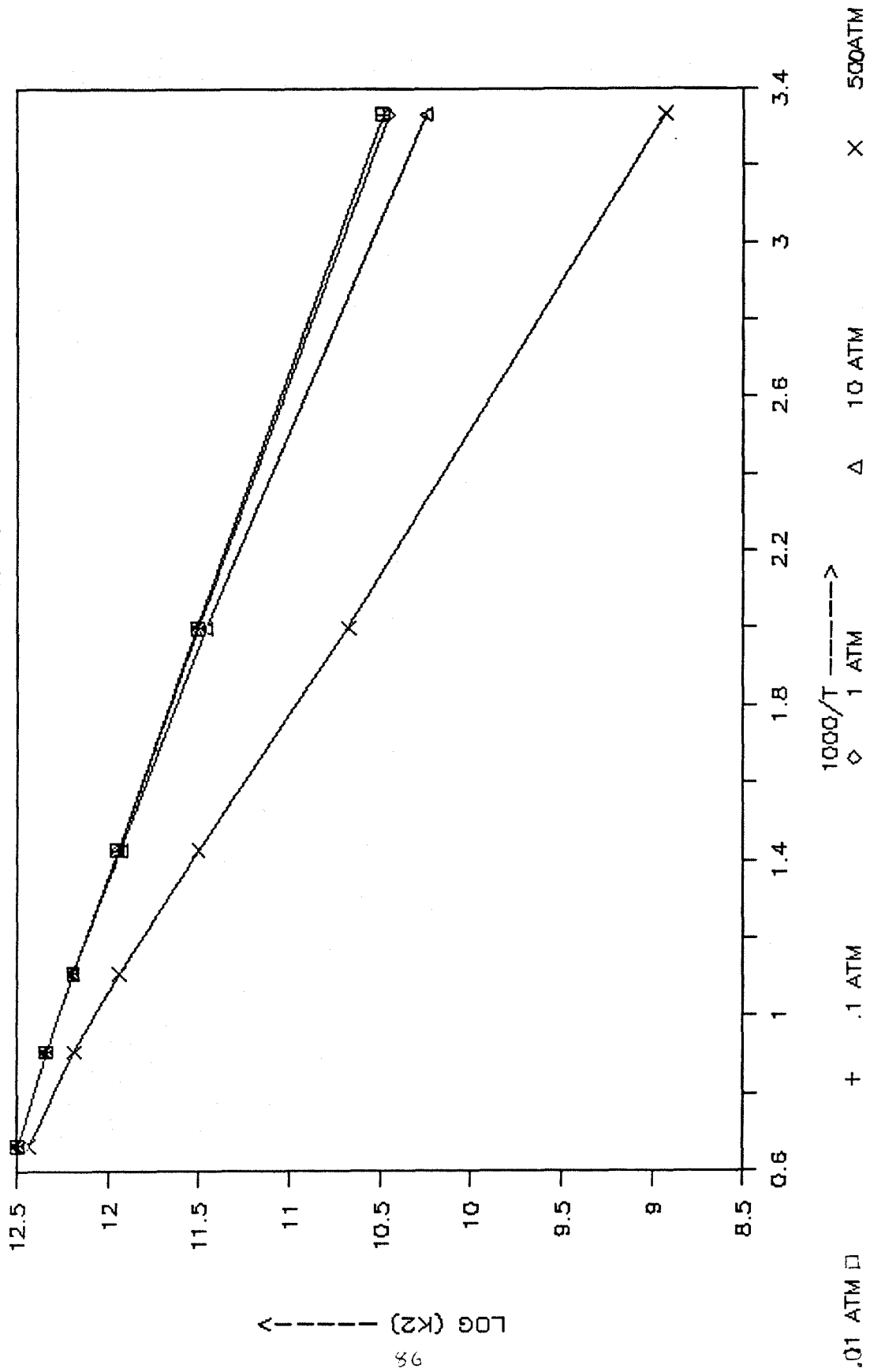
G4-A

O + CL BYPH. ETHER \longrightarrow (COMPLEX)s



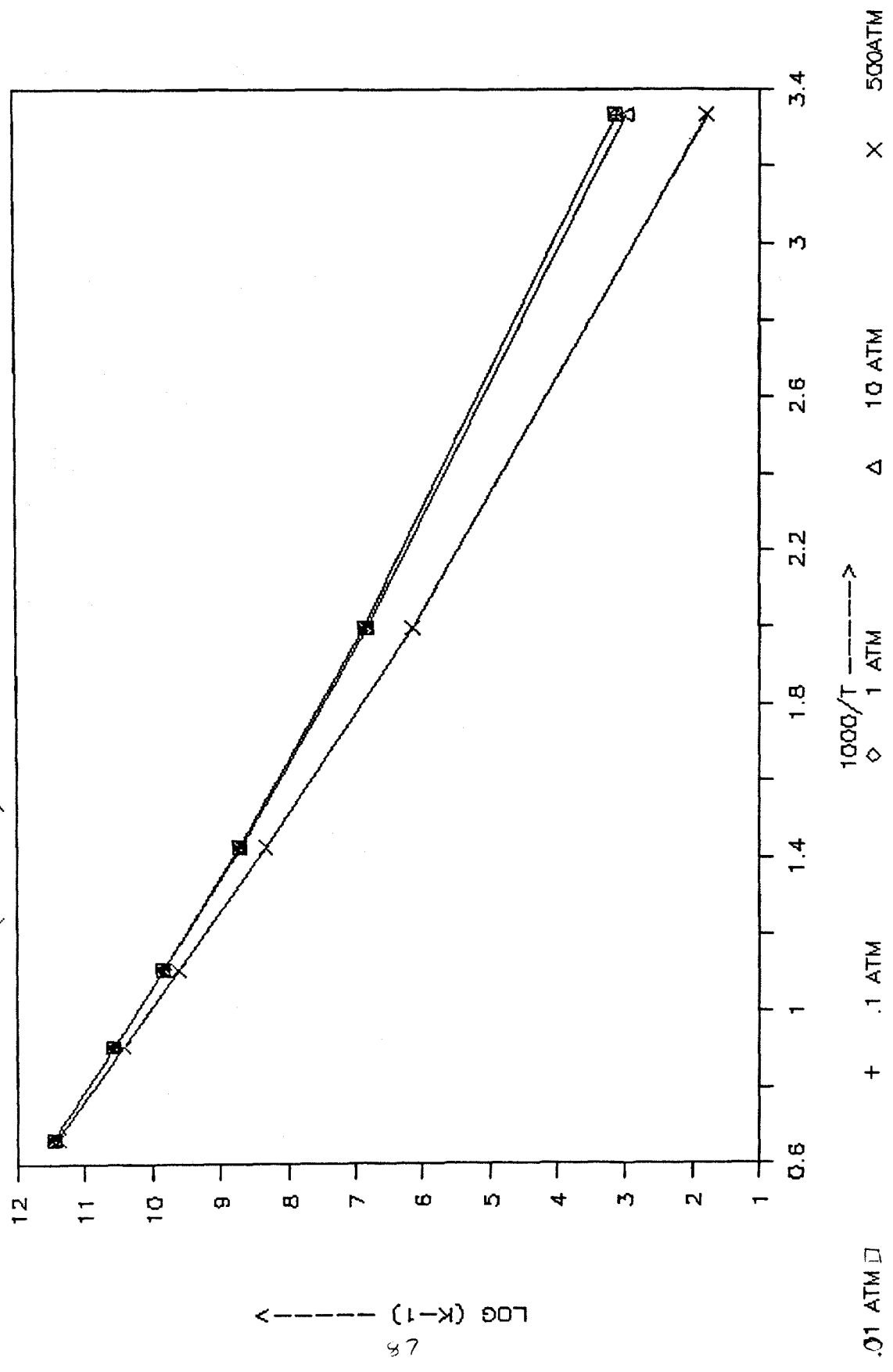
GRAPH G4-B

REACTANTS -----> PRODUCTS



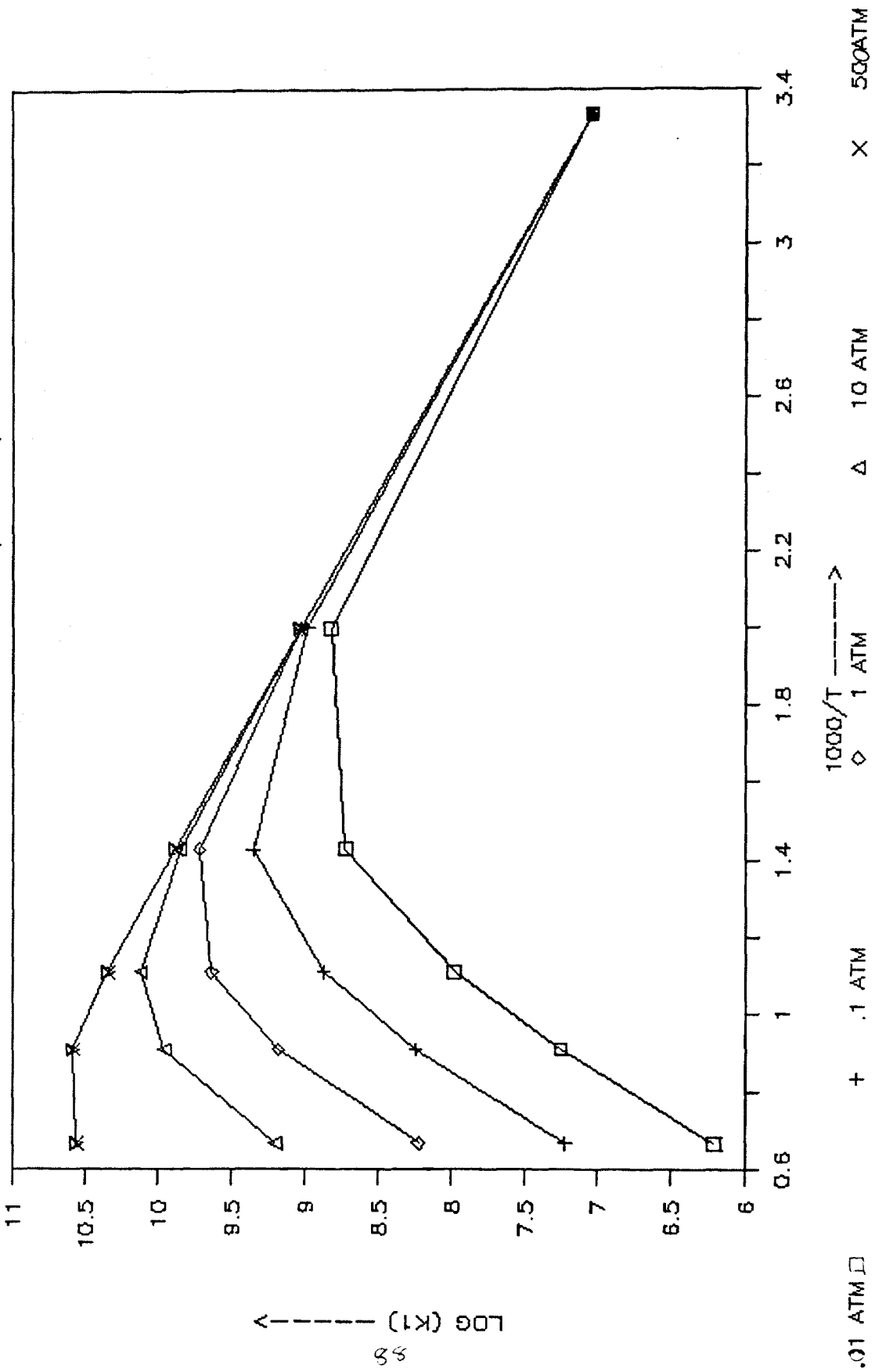
G4-C

(COMPLEX)e $\xrightarrow{\quad}$ O + Cl BYPH. ETHER



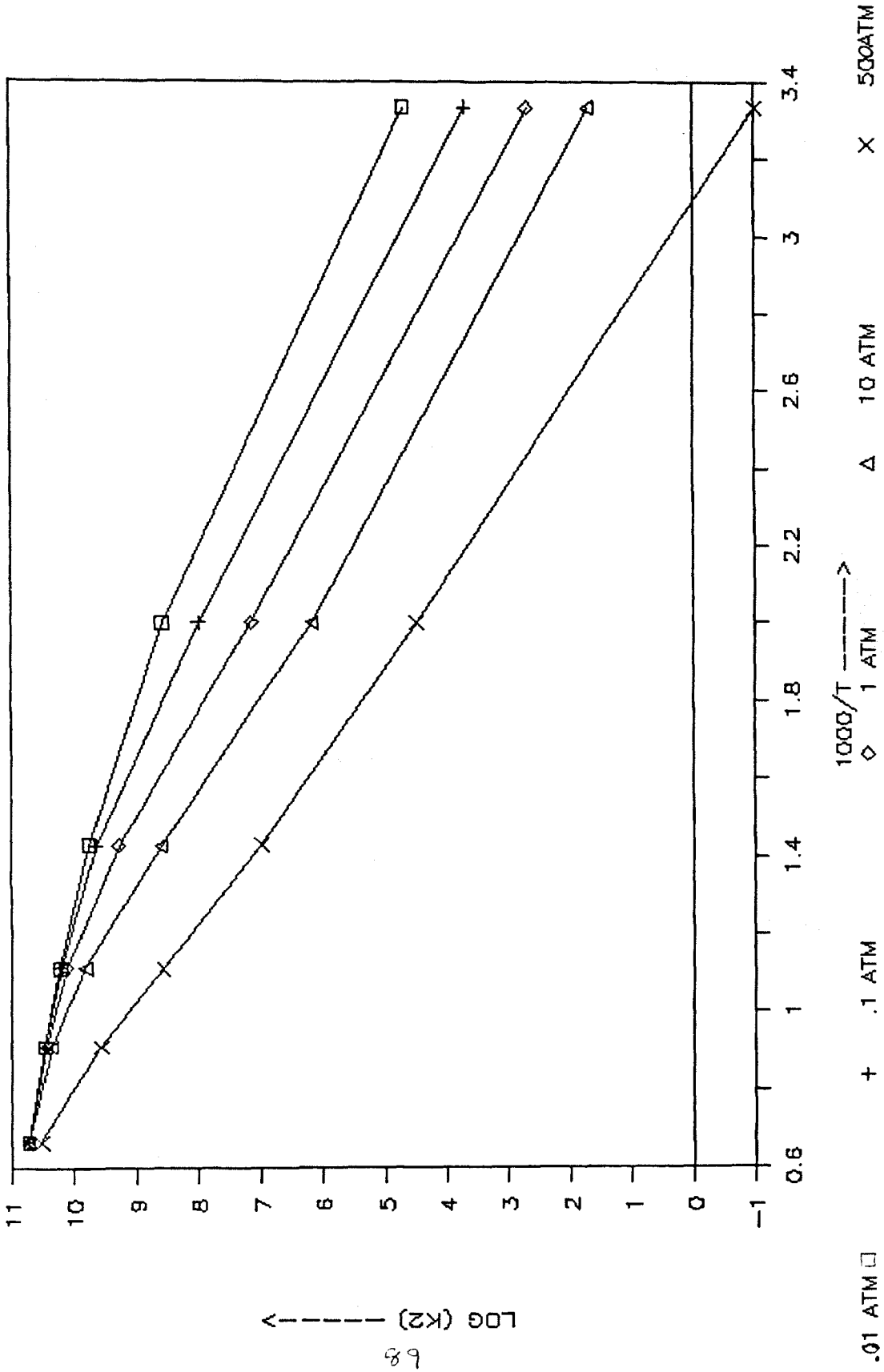
G5--A

Cl PH₂PHNXY. ETHER -----> (COMPLEX)s



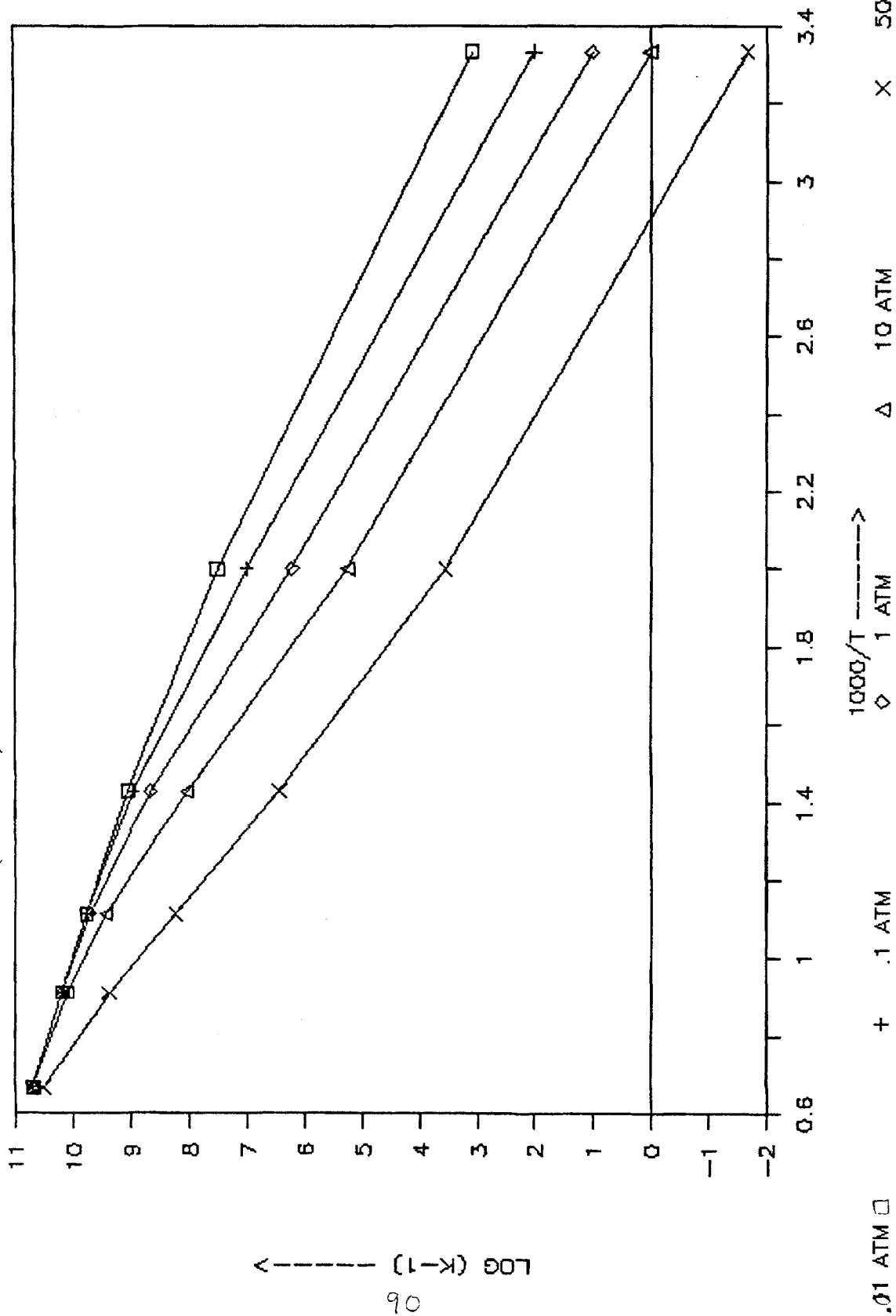
G5-B

CL PH. PHOXY ETHR \rightarrow CI + CI DIOXIN



G5-C

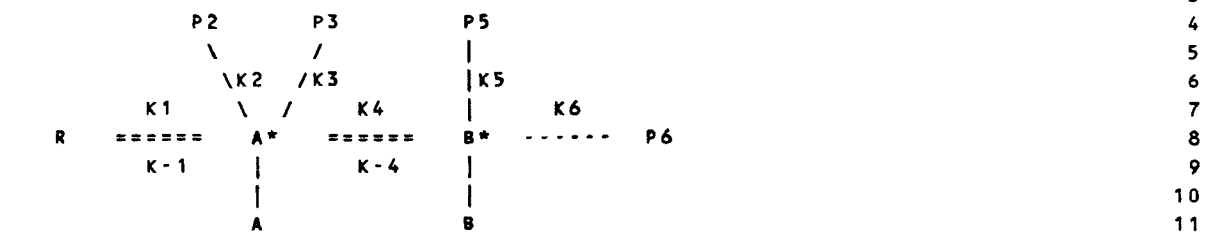
(COMPLEX)e -----> Cl PH. PHNXY ETHER



APPENDIX G

COMPUTER INPUTS FOR QRRK ANALYSIS

RECOMBINATION AND DECOMPOSITION (WITH ISOMERIZATION) USING QRRK



R (REACTANTS) 14
 phenoxy + tetrachloro benzene 15

A* (RECOMBINATION) P2 (1ST A* DECOMP) P3 (2ND A* DECOMP) 17
 C12H7CL40. C12H7CL30 CL 18

B* (ISOMER STABIL) P5 (1ST B* DECOMP) P6 (2ND B* DECOMP) 20

FREQ (FREQUENCY)(HZ) NS (WAVENUMBERS) 23
 604.46, 66, 24

HIGH PRESSURE RATE CONSTANT: A (M-CC-S) N E (KCAL) 26
 1.75E+12, 0.0, 4.0, 27

COLLISION COMPLEX MASS(A.U.) DIAMETER (A) WELL DEPTH (K) 29
 309.0, 7.0584, 599.54, 30

THIRD BODY 32
 AIR MASS (A.U.) DIAMETER (A) WELL DEPTH (CAL) ENERGY TRANS (CAL) 33
 28.89, 3.68, 113.423, 510.0, 34

A(M-CC-S)	E (KCAL)	
3.436E+14,	9.47,	K-1
3.33E+13,	5.17,	K2
0.0,	0.0,	K3
0.0,	0.0,	K4
0.0,	0.0,	K-4
0.0,	0.0,	K5
0.,	0.,	K6

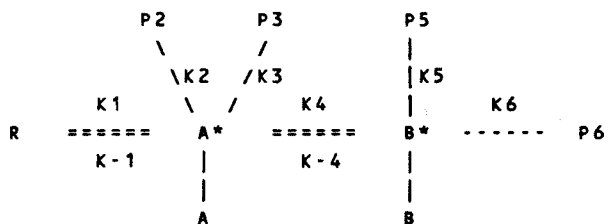
DELTA H FOR A* === B* (KCAL/MOL) XLAM (COLLISION COEFF) 51
 0.0, 0., 52

NUMBER OF TEMPERATURES T1 T2 T3 T4 T5 T6 (K) 54
 6, 300., 500., 700., 900., 1100., 1500., 55

							56
NUMBER OF PRESSURES	P1	P2	P3	P4	P5	P6 (TORR)	57
5,	7.6,	76.,	760.,	7600.,	38E+4,		58
							59
Tdist (FOR DISTRIBUTION Ki(E) vs. E AT THIS TEMP (K))							60
1100.,							61
							62
Pdist (FOR DISTRIBUTION Ki(E) vs. E AT THIS PRESS (TORR))							63
760,							64

Figure 12: Computer input for reaction represented in Figure 6

RECOMBINATION AND DECOMPOSITION (WITH ISOMERIZATION) USING QRRK



R (REACTANTS)

O + HEPTACHLORO BIPHENYL

A* (RECOMBINATION) P2 (1ST A* DECOMP) P3 (2ND A* DECOMP)
 C12H3CL7O. C12H2CL7O. + H

B* (ISOMER STABIL) P5 (1ST B* DECOMP) P6 (2ND B* DECOMP)

FREQ (FREQUENCY)(HZ) NS (WAVENUMBERS)
 578.06, 63,

HIGH PRESSURE RATE CONSTANT: A (M-CC-S) N E (KCAL)
 1.00E+13, 0.0, 3.5,

COLLISION COMPLEX MASS(A.U.) DIAMETER (A) WELL DEPTH (K)
 411.5, 6.39, 254.23,

THIRD BODY

AIR MASS (A.U.) DIAMETER (A) WELL DEPTH (CAL) ENERGY TRANS (CAL)
 28.89, 3.68, 113.423, 510.0,

A(M-CC-S)	E (KCAL)	
2.58E+13,	26.58,	K-1
1.58E+13,	4.00,	K2
0.0,	0.0,	K3
0.0,	0.0,	K4
0.0,	0.0,	K-4
0.0,	0.0,	K5
0.,	0.,	K6

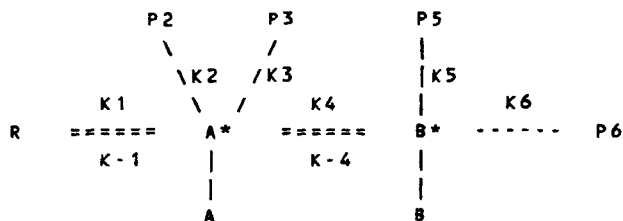
DELTA H FOR A* == B* (KCAL/MOL) XLAM (COLLISION COEFF)
 0.0, 0.,

NUMBER OF TEMPERATURES T1 T2 T3 T4 T5 T6 (K)
 6, 300., 500., 700., 900., 1100., 1500.,

NUMBER OF PRESSURES	P1	P2	P3	P4	P5	P6 (TORR)	56
5,	7.6,	76.,	760.,	7600.,	38E4,		57
							58
							59
Tdist (FOR DISTRIBUTION Ki(E) vs. E AT THIS TEMP (K))							60
1100.,							61
							62
Pdist (FOR DISTRIBUTION Ki(E) vs. E AT THIS PRESS (TORR))							63
760.,							64

Figure 13: Computer input for reaction represented in Figure 10

RECOMBINATION AND DECOMPOSITION (WITH ISOMERIZATION) USING QRRK



1
2
3
4
5
6
7
8
9
10
11
12
13
14
15
16
17
18
19
20
21
22
23
24
25
26
27
28
29
30
31
32
33
34
35
36
37
38
39
40
41
42
43
44
45
46
47
48
49
50
51
52
53
54
55

R (REACTANTS)
HEPTACHLORO PHENYLPHENOXY

A* (RECOMBINATION) P2 (1ST A* DECOMP) P3 (2ND A* DECOMP)
C12H2CL7O. C12H2CL6O + CL

B* (ISOMER STABIL) P5 (1ST B* DECOMP) P6 (2ND B* DECOMP)

FREQ (FREQUENCY)(HZ) NS (WAVENUMBERS)
737.823 63,

HIGH PRESSURE RATE CONSTANT: A (M-CC-S) N E (KCAL)
2.14E+12, 0.0, 8.73

COLLISION COMPLEX MASS(A.U.) DIAMETER (A) WELL DEPTH (K)
410.5, 7.0108, 851.821

THIRD BODY
AIR MASS (A.U.) DIAMETER (A) WELL DEPTH (CAL) ENERGY TRANS (CAL)
28.89, 3.68, 113.423, 510.0,

A(M-CC-S)	E (KCAL)	
1.953E+11,	11.24,	K-1
9.037E+11,	9.70,	K2
0.0,	0.0,	K3
0.0,	0.0,	K4
0.0,	0.0,	K-4
0.0,	0.0,	K5
0.,	0.,	K6

DELTA H FOR A* == B* (KCAL/MOL) XLAM (COLLISION COEFF)
0.0, 0.,

NUMBER OF TEMPERATURES	T1	T2	T3	T4	T5	T6 (K)
6,	300.,	500.,	700.,	900.,	1100.,	1500.,

NUMBER OF PRESSURES	P1	P2	P3	P4	P5	P6 (TORR)	56
5,	7.6,	76.,	760.,	7600.,	38E4,		57
							58
							59
Tdist (FOR DISTRIBUTION Ki(E) vs. E AT THIS TEMP (K))							60
1100.,							61
							62
Pdist (FOR DISTRIBUTION Ki(E) vs. E AT THIS PRESS (TORR))							63
760.,							64

Figure 14: Computer input for reaction represented in Figure 1

NUMBER OF PRESSURES	P1	P2	P3	P4	P5	P6 (TORR)	56
5,	7.6,	76.,	760.,	7600.,	38E4,		57
							58
							59
Tdist (FOR DISTRIBUTION Ki(E) vs. E AT THIS TEMP (K))							60
1100.,							61
							62
Pdist (FOR DISTRIBUTION Ki(E) vs. E AT THIS PRESS (TORR))							63
760.,							64

Figure 15: Computer input for figure represented in Figure 11

NUMBER OF PRESSURES	P1	P2	P3	P4	P5	P6 (TORR)	56
5,	7.6,	76.,	760.,	7600.,	38E4,		57
							58
							59
Tdist (FOR DISTRIBUTION $K_i(E)$ vs. E AT THIS TEMP (K))							60
1100.,							61
							62
Pdist (FOR DISTRIBUTION $K_i(E)$ vs. E AT THIS PRESS (TORR))							63
760.,							64

Figure 16: Computer input for reaction represented in Figure 3

APPENDIX H

SYNOPSIS FOR CHAPTERS I TO III

SYNOPSIS

Estimation of Ring Correction Groups

Ring correction groups for use in calculating thermodynamic properties H_f , S_f , and $Cp_{300-1000\text{ K}}$ have been determined for hydrocarbons, and oxygen, nitrogen and sulfur containing organic ring compounds. The ring groups calculated are used in conjunction with Benson's Group Additivity method for calculation of thermodynamic properties H_f^{298} , S_f^{298} , and $Cp_{300-1000\text{ K}}$ of these molecules. The data supplements the tables of these Benson Group values and permits estimation of the above thermodynamic properties of these ring compounds, which were not previously possible.

Estimation of group interaction terms for aromatic rings:

Correction terms or groups for multisubstitutes on the aromatic rings have been derived for use with the Benson Group Additivity method to predict accurate thermodynamic properties. Specific data have been determined for methyl, chloro, fluoro, hydroxy etc. substituents in ortho, meta and para positions. A calculation scheme has been proposed to estimate thermodynamic properties (enthalpy, entropy and heat capacities) when multiple substituents are present on the aromatic ring. Thermodynamic properties estimated using the ring substituent terms are compared with the literature data in addition to data using Benson Groups without

substituent correction terms.

Reaction pathways leading to the formation of Dioxins and dibenzofurans:

Aromatic ring substituent interactions previously determined for use with the Benson Group Additivity method of thermodynamic property estimation have been used to determine thermodynamic parameters and potential energy diagrams for likely pathways of chlorinated and nonchlorinated Dioxin formation. The thermodynamic data show that formation of chlorinated dioxins is significantly more favorable than the corresponding non chlorinated compounds. Plausible pathways are shown for which might lead to dioxin formation during incineration/oxidation of aromatics.

REFERENCES

- (1) S. W. Benson and J. H. Buss, *J. Chem. phys.*, **29**, 546 (1958).
- (2) Benson et al. *Chem Rev.*, **69**, 279 (1969).
- (3) S. W. Benson, *Thermochemical Kinetics*, John Wiley 1976.
- (4) O. V. Dorofeeva, L. V. Gurvich, V. S. Jorish, *J. Phys. Chem. Ref Data*, Vol15, # 2, 1986.
- (5) Ritter E. R., PhD Thesis, Department of Chemical Engineering, Chemistry and Environmental Science, New Jersey Institute of Technology (1989)
- (6) D. R. Stull, E. F. Westrum Jr. , G. C. Sinke, *The Chemical Thermodynamics of Organic Compounds*, Robert E. Krieger publishing company, Malabar Florida, 1987.
- (7) J. B. Pedley, R. D. Naylor and S. P. Kirby, *Thermochemical Data of Organic Compounds*, 2nd ed., Chapman & Hall, London 1986.
- (8) O. Hutzinger, M. J. Blumich, M.v.d. Berg and K. Olie, *Chemosphere*, Vol. **14**, No. 6/7, pp 581-600, 1985.
- (9) Kudchadker et. al., *J. Phys. Chem. Ref. Data*, vol 7, 2, 1978
- (10) M. D. M. C. Ribeiro Da Silva et. al., *J. Chem. Thermodynamics*, 1984, **16**, 1149-1155.
- (11) M. L. C. C. H. Ferrao, G. Pilcher, *J. Chem. Thermodynamics*, 1987, **19**, 543-548.
- (12) J. H. Green and D. J. Harrison, *J. Chem. Thermodynamics*, 1976, **8**, 529-544.
- (13) M. Colomina et. al., *J. Chem. Thermodynamics*, 1984, **16**, 1121-1127.
- (14) M. Colomina, P. Jimenez, M. V. Roux, C. Turrion, *J. Chem. Thermodynamics*, 1985, **17**, 1091-1096.
- (15) M. A. V. Ribeirio DA Silva, M. D. M. C. Ribeirio DA Silva and G. Pilcher, *J. Chem. Thermodynamics*, 1988, **20**, 969-974.

- (16) W. M. Shaub, *Thermochimica Acta*, **55** (1982), 59-73.
- (17) W. M. Shaub, *Thermochimica Acta*, **62** (1983) 315-323.
- (18) Francisco J. S., Williams I. H., *International Journal of Chemical Kinetics*, Vol. 20, 455-466 (1988).
- (19) J. A. Draeger, *J. Chem. Thermodynamics*, 1985, **17**, 263-275.
- (20) J. D. Cox, G. Pilcher, *Thermochemistry of Organic and Organometallic Compounds*, Academic Press, London 1970.
- (21) He. Y. Z., Mallard W. G., Tsang W., *J. Phys. Chem.* 1988, **92**, 2196-2201.
- (22) Dean A. M., *J. Phys. Chem.* 1985, **89**, p-4600.
- (23) Westmoreland P., Longwell J., Sarofim A. and Dean A. M., personal communication *J. Phys. Chem.* 1989, submitted.
- (24) Stein S., *J. Phys. Chem.*, 1978, **82**, pg-566.
- (25) Mckinna T., Howard J. and Longwell J., *Proceedings of the 22 International Combustion Institute*, Seattle, Washington, Aug. 1988.
- (26) Winer A. and Harris S., *Proceedings of the 22 International Combustion Institute*, Seattle, Washington, Aug. 1988.
- (27) *Chemosphere*, vol 16, No. 1, pp 29-36, 1987
- (28) National Dioxin Study Tier 4-combustion sources EPA-450/4-84-014g Sept. 1987
- (29) *Chemosphere*, vol 14, No. 6, pp 581-600, 1985
- (30) Dean A. M., *J. Phys. Chem.*, 1985, **89**, 4600
- (31) Westmoreland P. R.; Howard J. B.; Longwell J. P.; Dean A. M., *AIChE J.* 1986, **32**, 1971
- (32) Kassel, L. S., *J. Phys. Chem.* 1982, **32**, 225, 1065
- (33) Troe J., *J. Chem. Phys.* 1977, **66**, 4745-4748
- (34) Troe J., *J. Phys. Chem.* 1979, **83**, 114
- (35) Troe J., *J. Chem. Phys.* 1981, **75**, 226
- (36) Gardiner Jr. W. C., *Combustion Chemistry*; Gardiner Jr. W. C., Ed. Springer Verlag: New York, 1984

- (37) Handbook of bimolecular and termolecular reactions;
Kerr J. A., Moss S. J., CRC Press: Boca Raton FL, 1981;
Vol I and II
- (38) Herron J. T. and Huie R. E. J. Phys. Chem. Ref.
Data, Vol 2, No. 3, 1973.
- (39) Robaugh D. A. and Stein S. E., J. Am. Chem. Soc.,
1986, 108, 3224-3229.
- (40) Stein S. E. and Golden D. M., J. Org. Chem., Vol 42,
No. 5, 1977.